# Generalized corresponding states model for bulk and interfacial properties in pure fluids and fluid mixtures

S. B. Kiselev[a] and J. F. Ely
*Chemical Engineering Department, Colorado School of Mines, Golden, Colorado 80401-1887*

(Received 13 March 2003; accepted 9 July 2003)

We have formulated a general approach for transforming an analytical equation of state (EOS) into the crossover form and developed a generalized cubic (GC) EOS for pure fluids, which incorporates nonanalytic scaling laws in the critical region and in the limit $\rho \to 0$ is transformed into the ideal gas equation EOS. Using the GC EOS as a reference equation, we have developed a generalized version of the corresponding states (GCS) model, which contains the critical point parameters and accentric factor as input as well as the Ginzburg number Gi. For nonionic fluids we propose a simple correlation between the Ginzburg number Gi and $Z_c$, $\omega$, and molecular weight $M_w$. In the second step, we develop on the basis of the GCS model and the density functional theory a GCS-density functional theory (DFT) crossover model for the vapor–liquid interface and surface tension. We use the GCS-DFT model for the prediction of the PVT, vapor–liquid equilibrium (VLE) and surface properties of more than 30 pure fluids. In a wide range of thermodynamic states, including the nearest vicinity of the critical point, the GCS reproduces the PVT and VLE surface and the surface tension of one-component fluids (polar and nonpolar) with high accuracy. In the critical region, the GCS-DFT predictions for the surface tension are in excellent agreement with experimental data and theoretical renormalization-group model developed earlier. Using the principle of the critical-point universality we extended the GCS-DFT model to fluid mixtures and developed a field-variable based GCS-FV model. We provide extensive comparisons of the GCS-FV model with experimental data and with the GCS-XV model formulated in terms of the conventional density variable—composition. Far from the critical point both models, GCS-FV and GCS-XV, give practically similar results, but in the critical region, the GCS-FV model yields a better representation of the VLE surface of binary mixtures than the GCS-XV model. We also show that by considering the Ginzburg number Gi as an independent CS parameter the GCS model is capable of reproducing the phase behavior of finite neutral nuclear matter. © *2003 American Institute of Physics.*
[DOI: 10.1063/1.1605375]

## I. INTRODUCTION

In recent years, there has been a substantial interest in supercritical fluids (SCFs) from both the academic and industrial communities.[1] One important issue is to replace or reduce the use of organic solvents[2–4] with sub- and supercritical liquids such as water[5–8] and carbon dioxide.[9–13] To make the potential for SCF technology more effective, it is imperative to have a consistent thermodynamic model of SCF solution behavior, capable of giving a good representation not only for vapor–liquid equilibrium (VLE) and PVT properties, but also of their many derivatives and interface. For nonideal systems, like those containing supercritical fluids, this is a challenging task by itself. The classical solution of this problem was first given by van der Waals (vdW),[14] who proposed a simple cubic equation of state (EOS) based on the ideal gas equation as a zeroth approximation, and including the effects of intermolecular interaction to a first approximation. The vdW EOS is the simplest equation, which predicts the existence of the critical point and yields a qualitative prediction of vapor–liquid equilibrium in real fluids. It also allows an explicit formulation of the corresponding states (CS) principle. However, the van der Waals EOS and CS model are qualitatively correct only for systems with two-parameter spherically symmetric intermolecular potentials.[15] The quantitative difference between theory and experiment in real molecular fluids is rather substantial, especially in the critical region. The first well-known attempts to improve the vdW EOS were made by Redlich and Kwong,[16] Soave,[17] and Peng and Robinson.[18] These equations of state, and their different empirical and semiempirical modifications (for a review see Ref. 19) yield a much better representation of the thermodynamic properties of fluids and fluid mixtures than the original vdW EOS. However, all these models thermodynamically are not self-consistent. Namely, they cannot describe different thermodynamic properties such as VLE, PVT, densities, specific heats, enthalpies, and excess properties in the gas and liquid phases simultaneously with the same set of the system-dependent parameters. Besides, all these analytical equations of state fail to reproduce the nonanalytical, singular behavior of fluids in the critical region, which are caused by long-scale fluctuations in density.

The thermodynamic properties of pure fluids in the criti-

[a]Author to whom all correspondence should be addressed. Electronic mail: skiselev@mines.edu

 

cal region can be described correctly with the so-called scaled EOS.[20] However, in the limit of low densities, even in the crossover formulation,[21] the scaled EOS do not reduce to the ideal gas EOS. Therefore, during the last two decades many efforts have been made to develop the ''global,'' or renormalized EOS that at low densities reproduce the ideal gas equation and is transformed into the nonanalytic scaled EOS as the critical point is approached.[22–48] The most recent and theoretically well founded are the hierarchical reference theory (HRT) developed by Parola and co-workers[24–28] and the ''globalized'' renormalization-group (RG) procedure proposed by White and co-workers.[36–40] A big advantage of the HRT[24–28] and ''globalized'' RG[36–40] models is that they require only few microscopic intermolecular potential parameters as input. The price for this is tedious calculations related to an implementation of these first-principle theoretical models. White's ''globalized'' RG model,[36–40] for example, similar to the MSA+RG model by Tang[43] and EOSCF +RG model by Prausnitz and co-workers[44–49] can be solved only numerically and requires additional spline functions for the representation of the thermodynamic surface of real fluids. This restricts their widespread practical application, especially for the critical mixtures where two-phase equilibrium calculations require the smaller steps and larger number of iterations for their convergence. Another shortcoming of the EOSCF+RG model developed by Jiang and Prausnitz[48,49] is that for mixtures it was formulated in terms of the ''density'' variable—composition, that in the critical region is, rigorously speaking, incorrect.

The thermodynamic surface of fluid mixtures in the critical region differs substantially from that of pure fluids.[50–52] According to the principle of critical-point universality,[53–55] also called the isomorphism principle,[56,57] a critical mixture exhibits pure fluid like singularities at fixed ''field'' variable—the chemical potential, rather than at fixed ''density'' variable—the composition. There are few crossover models of mixtures that incorporate scaling laws in the critical region and transform into an analytical equation of state far away from the critical point. Examples include the field-space conformal model based on the modified Peng–Robinson and Benedict–Webb–Rubin EOS,[23,58] the six-term crossover model,[59–63] the crossover Leung–Griffiths (CR LG) model,[64,65] and the more extensive parametric crossover model developed by Kiselev and co-workers.[66–71] The Helmholtz free-energy in the latter model, also known as CREOS-97,[66] was represented in a universal parametric form, which does not depend on the detail of the intermolecular interactions and is equally valid for any pure fluid and binary mixture in the critical region, including aqueous ionic solutions. Recently, the parametric crossover models, named by CREOS-01 and CREOS-02, have been applied to the description of the thermodynamic properties of supercooled liquid $H_2O$, $D_2O$, and $H_2O+D_2O$ mixtures,[72,73] respectively. However, CREOS-97 (as are CREOS-01 and CREOS-02) is an asymptotic crossover model,[21] which fails to reproduce the ideal gas equation in the limit of low densities.

A more general, phenomenological procedure for incorporating of the long-range density fluctuations into any classical equation was proposed by Kiselev.[74] This procedure is based on the renormalization-group theory and can be applied to any analytical EOS, which predicts a critical point and in the limit of low densities is transformed into the ideal gas equation. An advantage of Kiselev's approach is that the crossover expression for the Helmholtz free energy in this approach can be written in the closed analytical form, which allows an analytical formulation of all derivatives. Kiselev's approach has been successfully applied for the cubic,[74,75] SAFT,[76–80] SAFT-BACK,[81] and high accuracy semiempirical EOS for square-well fluids.[82] In all cases, this method produces a thermodynamically self-consistent and accurate crossover EOS near to and far from the critical point of pure fluids[74,75,83] and fluid mixtures.[78,83] However, the crossover EOS in this approach contains four more adjustable parameters than an original classical EOS, and similar to the EOSCF+RG model,[48,49] they have been applied so far only in the density-variable formulation for mixtures.

In this paper we continue a study initiated in our previous works for the cubic[74,83] and SAFT[76–79] EOS. Using the crossover sine model,[78] we develop a generalized cubic (GC) EOS, which unlike the cubic crossover EOS developed before, can be analytically extended into the metastable region and reproduces analytically connected van der Waals loops. Second, we developed on the basis of the GC EOS and the density functional theory (DFT) a GCS-DFT model for bulk properties and surface tension. We use this model for the prediction of the volumetric, VLE properties and surface tension of more than 30 (polar and nonpolar) pure fluids in a wide range of the parameters of state, including the nearest vicinity of the critical point. Combining the GCS model with the principle of critical-point universality we have also developed an isomorphic GCS for fluid mixtures, the GCS-FV model.

We proceed as follows: In Sec. II we describe a general procedure for transforming any analytical equation into the crossover form. In Sec. III we develop a crossover cubic EOS for pure fluids. In Sec. IV we developed the GCS model and applied this model for more than 30 pure fluids. We consider a generalized CS-DFT model for surface tension in Sec. V. In Sec. VI we consider an extension of the GCS model to fluid mixtures, and our results are summarized and discussed in Sec. VII.

## II. THEORETICAL BACKGROUND

The critical point in pure fluids is the simplest example of a second-order phase transition, and the vdW EOS in the critical region corresponds to the Landau, or mean-field, theory of the second-order phase transitions. In the Landau theory,[15] the critical part $\Delta F(T,\eta)$ of the thermodynamic potential of the system undergoing the second-order phase transition is represented in the powers of the order parameter $\eta$,

$$\Delta F(T,\eta)=a_0\tau\eta^2+u_0\eta^4-h\eta, \tag{2.1}$$

where $\tau=T/T_c-1$ is a dimensionless deviation of the temperature $T$ from the transition temperature $T_c$, the coefficients $a_0>0$ and $u_0>0$ are the system-dependent parameters, and $h$ is an external ordering field. The term $\propto\eta^3$,

which breaks the symmetry of thermodynamic potential with respect to the transformation $h \to -h$ and $\eta \to -\eta$, was omitted in Eq. (2.1) because it can be effectively taken into account by simple redefinition of the order parameter $\eta \to \eta + d_1\tau$.[15,84] An equation of state, which corresponds to the thermodynamic potential (2.1) is given by

$$h = 2a_0\tau\eta + 4u_0\eta^3, \tag{2.2}$$

where $\eta = -\partial F(T,h)/\partial h$ is an equilibrium value of the order parameter.[15] After integration, the equilibrium thermodynamic potential of the system near the second-order phase transition in the Landau theory can be written in the form

$$F(T,\eta) = a_0\tau\eta^2 + u_0\eta^4 + F_{\mathrm{bg}}(T,\rho), \tag{2.3}$$

where the background contribution $F_{\mathrm{bg}}(T,\rho)$ is an analytic function of $T$ and $\rho$.

The Landau theory is valid only in the temperature region $\mathrm{Gi} \ll |\tau| \ll 1$ where the long-scale fluctuations in the order parameter are small.[15,84] Here $\mathrm{Gi} \propto (u_0\nu_c/a_0^2\overline{\xi_0^3})^2$ is the Ginzburg number, $\nu_c$ is a critical volume, and $\overline{\xi}_0$ is an effective average radius of the interaction between molecules. The intensity of the fluctuations diverges at the critical point and, as a consequence, at temperatures $|\tau| \ll \mathrm{Gi}$ the singular part of the thermodynamic potential of a system becomes a nonanalytic function of the temperature $\tau$ and the order parameter $\eta$,

$$\Delta F(\tau,\eta) = A_0|\tau|^{2-a}\Psi_0(z), \tag{2.4}$$

where $\Psi_0(z)$ is a universal scaled function of the scaling argument $z = \eta/|\tau|^{\beta}$.

The crossover behavior of the thermodynamic potential of the system from the analytic Landau expansion (2.3) into the scaled equation (2.4) in the asymptotic critical region, also named the asymptotic crossover problem,[21] has been addressed with different theoretical methods by many authors[85–98] (for a review see Refs. 21 and 51). According to a general solution of the renormalization-group equations,[85–90] close to the critical point the fluctuations renormalize the dimensionless temperature $\tau$ and order parameter $\eta$ in the singular part of the thermodynamic potential (2.3), such that they become nonanalytic functions of $\tau$ and $\eta$,

$$\tau \to \overline{\tau} = \tau\Upsilon^{-a/2\Delta_1}, \quad \eta \to \overline{\eta} = \eta\Upsilon^{(\gamma-2\beta)/4\Delta_1}, \tag{2.5}$$

and Eq. (2.3) takes a form

$$\Delta F(\tau,\eta) = a_0\tau\Upsilon^{-\alpha/2\Delta_1}\eta^2\Upsilon^{(\gamma-2\beta)/2\Delta_1} + u_0\eta^4\Upsilon^{(\gamma-2\beta)/\Delta_1} - \mathrm{K}(\tau), \tag{2.6}$$

where $\alpha = 0.11$, $\beta = 0.325$, $\gamma = 2 - 2\beta - \alpha = 1.24$, and $\Delta_1 = 0.51$ are universal nonclassical critical exponents,[20,51] and $\Upsilon(\tau,\eta)$ denotes a crossover function. In Eq. (2.6) $\mathrm{K}(\tau)$ is a fluctuation induced kernel term,[85–90] which is responsible for the asymptotic singular behavior of the heat capacity in the zero external field $h = 0$, or $\eta = 0$ at $\tau > 0$,

$$C_V(\tau)/R = -\frac{T}{R}\left(\frac{\partial^2 F}{\partial T^2}\right)_{\eta=0} = A_0^{\pm}|\tau|^{-\alpha}(1 + a_1^{\pm}|\tau|^{\Delta_1}) + B_0^{\pm}(\tau), \tag{2.7}$$

where $A_0^{\pm}$ is the asymptotic amplitude, $a_1^{\pm}$ is the first Wegner-correction term,[99] and $B_0^{\pm}(\tau)$ is a background contribution above $(+)$ and below $(-)$ critical temperature. With this in mind, the kernel term can be written in the form[74]

$$K(\tau,\eta) = \tfrac{1}{2}a_{20}\tau^2[\Upsilon^{-\alpha/\Delta_1}(\tau,\eta) - 1] + \tfrac{1}{2}a_{21}\tau^2[\Upsilon^{-(\alpha-\Delta_1)/\Delta_1}(\tau,\eta) - 1], \tag{2.8}$$

where the coefficients $a_{20}$ and $a_{21}$ correspond to the asymptotic and first Wegner-correction terms in Eq. (2.7), respectively. At $\mathrm{Gi} \ll |\tau| \ll 1$ the crossover function $\Upsilon \cong 1$, and Eq. (2.7) becomes identical to the Landau expansion (2.3), while asymptotically close to the critical point, at $|\tau| \ll \mathrm{Gi}$, the crossover function $\Upsilon$ modifies each term in Eq. (2.6) in such a way that the singular part $\Delta F(\tau,\overline{\eta})$ is transformed into the scaled equation (2.4).

Mathematically, Eq. (2.1) corresponds to the asymptotic terms in the Taylor expansion of the thermodynamic potential of the system near the critical point $\tau = \eta = 0$ in the powers of $\tau$ and $\eta$.[15] In principle, as more terms are taken into account in Eq. (2.1), and consequently in expansion (2.6), a higher accuracy and wider range of temperatures and densities can be achieved with this crossover model. In pure fluids, except for the above-mentioned cubic term, additional asymmetric terms $\propto \eta^2 h$ and $\propto \eta$,[5] and the higher order symmetric terms $\propto \tau\eta^4$ and $\propto \tau^2\eta^2$, should be added into the expansion (2.7). As a consequence, the corresponding crossover model becomes more effective and accurate.[100–105]

The effectiveness of the crossover model is determined by the choice of the crossover function $\Upsilon$. Unfortunately, the RG equations for the crossover function $\Upsilon$ in real three-dimensional space can be solved rigorously only numerically. Therefore, in practice for the crossover function $\Upsilon$ different approximants[94,105] and phenomenological expressions[70,100–102] are usually used. Incorporation of the empirically corrected crossover function into the six-term Landau expansion, for example, has enabled this model to represent the thermodynamic properties of pure fluids[59,62,63] in a much wider range of the temperatures and densities than the two- and six-term Landau model of Chen *et al.*[103,104] based on the spherical-model crossover function phenomenologically repaired for the scalar order parameter by Nicoll and co-workers.[88–90] CREOS-97,[66–71,102] on the other hand, represents the thermodynamic surface of pure fluids even in a bigger temperature range (up to $T = 2T_c$) than the six-term Landau model,[59,62,63] but with the crossover function obtained by Kiselev[100] as a simple Pade-approximant of the numerical solution of the RG equations.[91–93] However, even with a well-determined crossover function $\Upsilon$, the extended Taylor expansion (2.6) diverges at $\rho \to 0$, and, therefore, in principle none of these crossover models can be used for developing a ''global'' EOS.

In order to develop a "global" crossover EOS, which reproduces the ideal gas equation in the limit of low densities, one needs to start from a full analytical expression for the thermodynamic potential

$$F(T,\rho)=F^{\mathrm{res}}(T,\rho)+F^{\mathrm{id}}(T,\rho), \tag{2.9}$$

where $F^{\mathrm{res}}(T,\rho)$ is the residual part and $F^{\mathrm{id}}(T,\rho)$ is the ideal gas contribution. Then one needs to replace the singular part $\Delta F(\tau,\eta)$ in Eq. (2.1) by the full expression obtained from Eq. (2.9)

$$\Delta F(\tau,\eta)=F(T,\rho)-F_{\mathrm{bg}}(T,\rho), \tag{2.10}$$

where for one-component fluids the background contribution $F_{\mathrm{bg}}(T,\rho)$ is an analytical function of temperature and density, to be specified in the following. The "global" crossover expression for the thermodynamic potential $F(T,\rho)$ in this case can be written in the form[74]

$$F(T,\rho)=\Delta F(\overline{\tau},\overline{\eta})-\mathrm{K}(\tau)+F_{\mathrm{bg}}(T,\rho), \tag{2.11}$$

where the renormalized parameters $\overline{\tau}$ and $\overline{\eta}$ are given by Eq. (2.5). In order to complete the transformation of the analytical thermodynamic potential $F(T,\rho)$ into the crossover form (2.11), one also needs to specify the crossover function $\Upsilon(\tau,\eta)$. The explicit expression $\Upsilon(\tau,\eta)$ in Kiselev's approach[74] is discussed in the following.

## III. CROSSOVER EQUATION OF STATE

In developing a generalized crossover EOS within the above-described theoretical approach, an important role belongs to the definition of the order parameter that determines which particular type of the thermodynamic potential should be used in Eq. (2.11). As was recently shown by Fisher *et al.*[106,107] neither the dimensionless density $\Delta\rho=\rho/\rho_c-1$ nor the molar volume $\Delta\nu=\nu/\nu_c-1$, but actually their linear combination should be used as the order parameter in one-component fluids. From the theoretical point of view, the choice of the order parameter determines which derivative $(\partial^2 P/\partial T^2)_{\rho_c}$ or $(\partial^2\mu/\partial T^2)_{\rho_c}$ is responsible for the divergence of the isochoric heat capacity at the critical point. In practice it appears that the VLE surface of a one-component fluid is more symmetric in $\Delta\rho$ variable, rather than in $\Delta\nu$.[108] Therefore, traditionally in all above-discussed asymptotic crossover models $\Delta\rho$ was used as the order parameter, and, as a consequence, in this case $(\partial^2 P/\partial T^2)_{\rho_c}\to\infty$ as $|\tau|\to 0$. For the GCS model this question becomes irrelevant because we set in this model the coefficients $a_{20}$ and $a_{21}$ in Eq. (2.8) equal to zero, and, therefore, both derivatives remain finite in the critical point. Therefore, following Kiselev,[74] we chose in the GCS model the dimensionless molar volume $\Delta\nu$ as the order parameter. Although $\Delta\nu$ is less symmetric in the critical region, it is better behaved over a broad range of state variables than the conventional density-based order parameter and at $\rho\to 0$ it naturally provides a physically obvious condition $\Upsilon=1$ in the dilute gas regime.

With $\Delta\nu$ as the order parameter, the thermodynamic potential $F(T,\rho)$ in Eq. (2.9) should be replaced by the classical expression for the dimensionless Helmholtz free energy $\overline{A}=A(T,\nu)/RT$ written in the form

$$\overline{A}(T,\nu)=\Delta\overline{A}(\Delta T,\Delta\nu)+\overline{A}_{\mathrm{bg}}(T,\nu), \tag{3.1}$$

where the critical part of the Helmholtz free energy

$$\Delta\overline{A}(\Delta T,\Delta\nu)=\overline{A}^{\mathrm{res}}(\Delta T,\Delta\nu)-\overline{A}^{\mathrm{res}}(\Delta T,0) -\ln(\Delta\nu+1)+\Delta\nu\overline{P}_0(\Delta T) \tag{3.2}$$

and the background contribution is given by

$$\overline{A}_{\mathrm{bg}}(T,\nu)=-\Delta\nu\overline{P}_0(T)+\overline{A}_0^{\mathrm{res}}(T)+\overline{A}^{\mathrm{id}}(T). \tag{3.3}$$

In Eqs. (3.1)–(3.3), $\Delta T=T/T_{0c}-1$ and $\Delta\nu=\nu/\nu_{0c}-1$ are dimensionless distances from the classical critical temperature $T_{0c}$ and molar volume $\nu_{0c}$, respectively, $\overline{P}_0(T)=P(T,\nu_{0c})\nu_{0c}/RT$ is the dimensionless pressure and $\overline{A}_0^{\mathrm{res}}(T)=\overline{A}^{\mathrm{res}}(T,\nu_{0c})$ is the dimensionless residual part of the Helmholtz energy along the critical isochore $\nu=\nu_{0c}$. $\overline{A}^{\mathrm{id}}(T)$ is the dimensionless temperature-dependent ideal-gas Helmholtz free energy.

In the next step, we need to replace the classical values of $\Delta T$ and $\Delta\nu$ in the critical part $\Delta\overline{A}(\Delta T,\Delta\nu)$ with the renormalized values $\overline{\tau}$ and $\overline{\eta}$. In the case where the classical critical parameters $T_{0c}$ and $\nu_{0c}$ determined from Eq. (A3) coincide with the real critical parameters $T_c$ and $\nu_c$, the renormalization $\Delta T\to\overline{\tau}$ and $\Delta\nu\to\overline{\eta}$ is given by Eq. (2.5). For some cubic EOS[109,110] the condition $T_{0c}=T_c$ can in principle be satisfied. However, in order to provide a better description of the vapor pressures and saturated liquid densities at low temperatures, for all cubic EOS the classical critical molar volume $\nu_{0c}$ is usually chosen to be bigger than the real critical molar volume $\nu_c$ (or $\rho_{0c}<\rho_c$).[111,112] In this work, a difference between real and classical critical volumes was effectively taken into account by incorporating into Eq. (2.5) the renormalized order parameter $\overline{\eta}$ additional term

$$\begin{aligned}\overline{\tau}&=\tau\Upsilon^{-\alpha/2\Delta_1},\\ \overline{\eta}&=\eta\Upsilon^{(\gamma-2\beta)/4\Delta_1}+(1+\eta)\Delta\nu_c\Upsilon^{(2-a)/2\Delta_1},\end{aligned} \tag{3.4}$$

where $\tau=T/T_c-1$ is a dimensionless deviation of the temperature from the real critical temperature $T_c$, $\eta=\nu/\nu_c-1$ is a dimensionless deviation of the molar volume form the real critical molar volume $\nu_c$, and $\Delta\nu_c=(\nu_c-\nu_{0c})/\nu_{0c}\ll 1$ is a dimensionless shift of the critical volume. The exponent $(2-\alpha)/2\Delta_1$ for the crossover function $\Upsilon$ in the second term in Eq. (3.4) has been obtained from the condition $\lim_{\tau\to 0}(\partial^2\overline{\eta}^2/\partial\tau^2)_{\eta=0}\propto\tau^{-\alpha}$. In this case, the corrections to the asymptotic singular behavior of the isochoric heat capacity $\delta C_V^{(1)}\propto\Delta\nu_c^2\tau^{(2-\alpha)/2}\approx\Delta\nu_c^2\tau$ and $\delta C_V^{(2)}\propto\Delta\nu_c^4\tau^{2(1-\alpha)}\approx\Delta\nu_c^4\tau^2$, which appear in Eq. (2.7) from this term at $\eta=0$, are a higher order of magnitude comparing the asymptotic, $\propto\tau^{-\alpha}$, and the first Wegner correction, $\propto\tau^{\Delta_1-\alpha}$, terms. Asymptotically close to the critical point, the crossover function $\Upsilon\to 0$, the term $\propto\Delta\nu_c\Upsilon^{(2-\alpha)/2\Delta_1}$ becomes negligibly small in comparison with the main term $\propto\eta\Upsilon^{(\gamma-2\beta)/4\Delta_1}$, and Eq. (3.4) is transformed into the original Eq. (2.5). Far away from the critical point $\Upsilon=1$ and the renoramalized order parameter $\overline{\eta}=\eta+(1+\eta)\Delta\nu_c=\nu/\nu_{0c}-1$ coincides with the classical order parameter $\Delta\nu$.

Since the RG equations cannot be solved analytically, no rigorous theoretical expression for the crossover function can be obtained by this method. Therefore, in practice different approximants are used for $\Upsilon$. The simplest one is a phenomenological crossover function obtained by Kiselev *et al.*,[74,76,83]

$$\Upsilon(q)=\left(\frac{q}{1+q}\right)^{2\Delta_1}, \tag{3.5}$$

where $q=(r/\mathrm{Gi})^{1/2}$ is a renormalized distance to the critical point and $r(\tau,\eta)$ is a parametric variable. The crossover function $\Upsilon$ given by Eq. (3.5) coincides with the corresponding crossover function in the CR LG model obtained in the first order of $\varepsilon$ expansion by Belyakov *et al.*[64] In our previous works,[74,76] the renormalized distance $q$ was found from a solution of the crossover linear model (LM). In this study, following our recent works[77–79] we find $q$ from a solution of the crossover sine model (SM)

$$\left(q^2-\frac{\tau}{\mathrm{Gi}}\right)\left[1-\frac{p^2}{4b^2}\left(1-\frac{\tau}{q^2\mathrm{Gi}}\right)\right] = b^2\left\{\frac{\eta[1+\nu_1\exp(-10\eta)]+d_1\tau}{m_0\mathrm{Gi}^{\beta}}\right\}^2\Upsilon^{(1-2\beta)/\Delta_1}, \tag{3.6}$$

where $m_0$, $\nu_1$, $d_1$, and Gi are the system-dependent parameters, while the universal parameters $p^2$ and $b^2$ can be set equal to the LM parameter $b^2_{\mathrm{LM}}=1.359$.[78] The term $\propto d_1\tau$ in Eq. (3.6) corresponds to the rectilinear diameter of the coexistence curve, which appears from the cubic term in the Landau expansion (2.1), as discussed earlier. At $|\eta|<0.5$, the linear-model crossover equation for the parametric variable $q$ employed earlier by Kiselev *et al.*[66,70,100,102] is recaptured from Eq. (3.6) when parameter $p^2\to 0$, while at $p^2>0$ Eq. (3.6) asymptotically close to the critical point ($q\ll 1$) is transformed into the trigonometric model originally developed by Fisher and co-workers.[113]

The RG theory equations (2.5) and (2.6) are, rigorously speaking, valid only in the region where the short-wavelength components of the order parameter can be excluded from consideration and the system can be statistically described with the effective Hamiltonian written in terms of the long-wavelength components only.[15,84] At the triple point of a liquid, the long-wavelength fluctuations are negligibly small, the RG theory is not applicable anymore, and the properties of the system should be described by the partition function with the microscopic Hamiltonian. As a consequence, the thermodynamic potential of liquid near the triple point is an analytical function of temperature and density. However, as was pointed out by Landau and Lifshitz,[15] because of the strong interaction between molecules a general calculation of the thermodynamic quantities in liquids, or even their temperature dependence, is impossible. The perturbation theory developed by Barker and Henderson[114] brings some relief in this grim prophecy of Landau and Lifshitz, but this analytical theory is not valid in the critical region. Therefore, we do not believe that any theoretical crossover expression for the thermodynamic potential of dense fluids can be obtained analytically. In this work, in order to provide a physically obvious condition $\Upsilon=1$ at the triple point of liquids, we added into the right-hand side of Eq. (3.6) an empirical term $\propto\nu_1\exp(-10\eta)$, where the coefficient $\nu_1$ is supposed to be positive and small ($0\leqslant\nu_1\ll 1$). This term is relevant only in dense liquids at $\rho>2\rho_c$ (or $\eta<-0.5$) where $\exp(-10\eta)\gg 1$. In the asymptotic critical and low-density regions this term is negligibly small and practically disappears at $\rho\to 0$ (or $\eta\to\infty$).

Finally, the crossover expression for the Helmholtz free energy can be written in the form

$$\overline{A}(T,\nu)=\Delta\overline{A}(\overline{\tau},\overline{\eta})-\mathrm{K}(\tau,\eta) -\Delta\nu\overline{P}_0(T)+\overline{A}_0^{\mathrm{res}}(T)+\overline{A}_{\mathrm{id}}(T) \tag{3.7}$$

with the kernel term given by Eq. (2.8). Asymptotically close to the critical point (at $q\ll 1$, or $|\tau|\ll\mathrm{Gi}$ at $\rho=\rho_c$ and $|\eta|\ll\mathrm{Gi}^{\beta}$ at $T=T_c$), the crossover function $\Upsilon\propto r^{\Delta_1}$, and the critical part $\Delta\overline{A}$ in Eq. (3.1) obeys the scaling low (2.4). In the intermediate region (at $q\sim 1$, or $|\tau|\sim\mathrm{Gi}<1$ and $|\eta|\sim\mathrm{Gi}^{\beta}<1$) $\Delta\overline{A}$ corresponds to the RG-theory expression (2.6), while far away from the critical point at $q\gg 1$ ($|\tau|\gg\mathrm{Gi}$ at $\rho=\rho_c$, or $|\eta|\gg\mathrm{Gi}^{\beta}$ at $T=T_c$) the crossover function $\Upsilon\to 1$ and Eq. (3.7) is transformed into the classical Helmholtz free energy (3.1). The GC EOS can be obtained by differentiation of Eq. (3.7) with respect to volume

$$P(\nu,T)=-RT\left(\frac{\partial\overline{A}}{\partial\nu}\right)_T =-\frac{RT}{\nu_{0c}}\left\{\frac{\nu_{0c}}{\nu_c}\left[\left(\frac{\partial\Delta\overline{A}}{\partial\eta}\right)_T+\left(\frac{\partial K}{\partial\eta}\right)_\tau\right]-\overline{P}_0(T)\right\}. \tag{3.8}$$

## IV. GENERALIZED CS MODEL FOR PURE FLUIDS

In developing the GCS model for a reference EOS we have chosen here a simple cubic Patel–Teja (PT) EOS.[109,110] The explicit form of the PT EROS and corresponding expressions for functions $\overline{A}^{\mathrm{res}}(\Delta T,\Delta\nu)$, $\overline{A}_0^{\mathrm{res}}(T)$, and $\overline{P}_0(T)$ for the PT EOS are given in Appendix A. The PT EOS is a good choice for developing a GCS model because by setting $b=c=0$ in the attractive term, it is transformed into the vdW EOS. With $b\neq 0$ and $c=0$ it corresponds to the Redlich–Kwong–Soave (RKS) EOS,[16,17] and choosing $b=c\neq 0$ the PT is transformed into the Peng–Robinson (PR) EOS.[18]

Written in the dimensionless form, the PT EOS corresponds to the four-parameter corresponding states model[109]

$$P_r=f_{\mathrm{PT}}(T_r,\rho_r;\omega,Z_{0c}), \tag{4.1}$$

where $P_r=P/P_{0c}$ and $\omega$ is the Pitzer's accentric factor. However, as we mentioned earlier, the CS models based on simple cubic equations of state give only a qualitative description of the thermodynamic surface of pure fluids, quantitatively their prediction is very bad. This is issue not only for the PT EOS, but also all other classical cubic EOS.[19] To provide an accurate representation, purpose, a complex EOS in combination with extended corresponding states principle is usually used.[115] In order to overcome this shortcoming of the cubic EOS, we develop here a generalized CS model, which requires the same number of the input parameters as

the classical CS model (4.1), but reproduces the PVT surface of one-component fluids with the much higher accuracy than the classical cubic EOS.

With this in mind, we will use for the function $\alpha_a(T_r)$ in Eq. (A2) the CS expression proposed by Jechura[116]

$$\alpha_a(T_r)=1+\Theta^2(T_r-1)-2\Theta(1+\Theta)(\sqrt{T_r}-1), \quad (4.2)$$

where the shape-factor is given by

$$\begin{aligned}\Theta=&11.9658\,Z_{0c}^3-7.224\,49\,Z_{0c}^2+4.938\,44\,Z_{0c}\\&-0.805\,807+(3.025\,16\,Z_{0c}+0.543\,518)\,\omega\\&-(0.428\,981\,Z_{0c}+1.520\,12\times10^{-2})\,\omega^2\\&+(3.795\,33\times10^{-2}\,Z_{0c}-1.812\,62\times10^{-4})\,\omega^3. \quad (4.3)\end{aligned}$$

In the PT EOS, $Z_{0c}$ is usually considered as an adjustable parameter, but in principle, it can be expressed as a function of $\omega$ and the real compressibility $Z_c$.[109] We found that for the GCS model a good approximation for $Z_{0c}$ is

$$Z_{0c}=\tfrac{1}{3}\tanh(-6.881\,56+1.465\,74\ \omega+32.8331\,Z_c), \quad (4.4)$$

where the pre-factor (1/3) before the hyperbolic tangent ensures for the PT EOS a requirement that at all $\omega$ and $Z_c$ the classical compressibility $Z_{0c}\leqslant 1/3$. Since even in the crossover formulation a simple cubic EOS is unable to reproduce $C_V$ data within an experimental accuracy,[74] we set in the GCS model the coefficients $a_{20}=a_{21}\equiv 0$, the coefficient $m_0=0.852$ was considered to be a system-independent parameter,[82] while the coefficients $d_1$ and $\nu_1$ were represented as functions of the critical compressibility

$$d_1=21.8356-83.425\,Z_c, \quad (4.5)$$

$$\nu_1=0.444\,163-3.613\,75\,Z_c+7.4084\,Z_c^2. \quad (4.6)$$

After this redefinition, the generalized corresponding state principle can be written in the form

$$P_r=f^{\mathrm{CR}}(T_r,\rho_r;\omega,Z_c,\mathrm{Gi}), \quad (4.7)$$

where $f^{\mathrm{CR}}$ for the PT EOS is determined by Eq. (3.8) with $\alpha_r$, $Z_{0c}$, $m_0$, $d_1$, and $\nu_1$ given by Eqs. (4.2)–(4.8), and the Ginzburg number is an additional CS parameter. Similar to the classical CS principle, the accentric factor $\omega$ in Eq. (4.7) determines the steepness of the vapor-pressure curve,[111] while the Ginzburg number Gi is responsible for the flatness of the vapor–liquid coexistence curve in the $\eta$–$\tau$ plane.[79] By definition, the Ginzburg number depends on the coefficients $a_0$ and $u_0$ in the Landau expansion (2.1), critical volume $\nu_c$, and the effective average radius of the interaction between molecules. In the critical region any EOS can be represented in the form of the Landau expansion (2.1), therefore, the coefficients $a_0$ and $u_0$, in principle, can be expressed as functions of $\omega$ and $Z_c$. Since in many nonionic fluids the critical volume $\nu_c$ directly related to the molecular weight $M_w$,[111] we assume that in these fluids the Ginzburg number can be also expressed as a function of $\omega$, $Z_c$, and $M_w$. Therefore, in order to make the GCS model more predictive, in the next step we represent the inverse Ginzburg number in the form

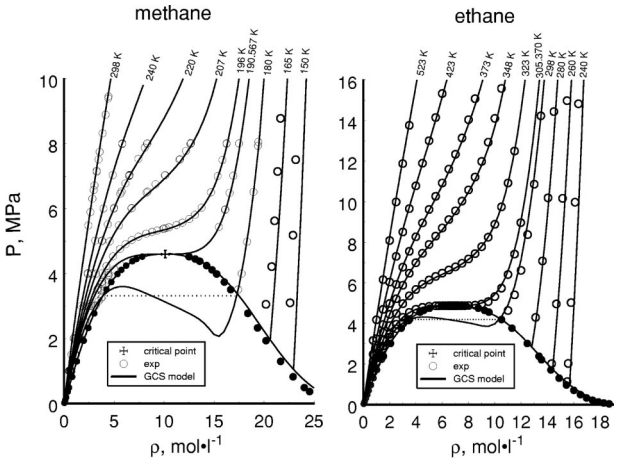


FIG. 1. $P\rho T$ data (symbols) for methane—Refs. 135–137 (left) and ethane—Ref. 138 (right) with predictions of the the GCS model (curves). The open symbols correspond to the one-phase region and the closed symbols indicate the VLE data.

$$\begin{aligned}\mathrm{Gi}^{-1}=&1.373\,55\times10^2\,\omega^{1/2}(1-2.189\,96\,\omega^{1/2}+1.769\,44\,\omega^{3/2})\\&+23.3958\,Z_c+4.883\,17\times10^{-2}\,M_w. \quad (4.8)\end{aligned}$$

Using Eq. (4.8), the GCS model for one-component nonionic fluids formally can be written in the classical form

$$P_r=f^{\mathrm{CR}}(T_r,\rho_r;\omega,Z_c) \quad (4.9)$$

where, however, unlike the classical CS model (4.1), the real critical parameters $T_c$, $\rho_c$, $Z_c$, and the crossover function $f^{\mathrm{CR}}$, instead of the classical function $f_{\mathrm{PT}}$, are used. In order to apply the GCS model to real fluids, similar to the classical CS model (4.1), one needs to know only the real critical parameters $T_c$, $\rho_c$, $Z_c$, and the accentric factor $\omega$.

The numerical values of all coefficients in Eqs. (4.4)–(4.8) have been found from an analysis of the PVT and VLE data for methane, ethane, carbon dioxide, water, and refrigerants R32, R125, and R134A. The predictions of the GCS model for methane, ethane, carbon dioxide, and water in comparison with experimental data are shown in Figs. 1 and 2. In general, very good agreement between the GCS model and experimental data for all four fluids is observed. We would especially like to emphasize the excellent agreement between experimental liquid- and vapor-density data and predictions of the GCS model in the critical region at $T_c\geqslant T\geqslant 0.9T_c$. Only at low temperatures $T\leqslant 0.6T_c$ for methane and water does the GCS model predict systematically higher (up to 3% for $CH_4$ and up to 7% for $H_2O$) values of liquid densities than the experimental data. But outside from this region, at $T\geqslant 0.6T_c$, the GCS model reproduces the saturated pressure and liquid density data for all fluids with an average absolute deviation (AAD) of about 1% and the vapor density with AAD of about 2–3%. In the one phase region at $\rho\leqslant 2\rho_c$ the GCS model reproduces the PVT data with an AAD less than 2% and the liquid densities at $\rho\geqslant 2\rho_c$ with an AAD of about 1–2%.

We should note that some simple EOS involving exponential attractive term, like a revised Dieterici–Carnahan–Starling (DCS) EOS developed recently by Sadus[117] for example, are also capable of representing the liquid–vapor

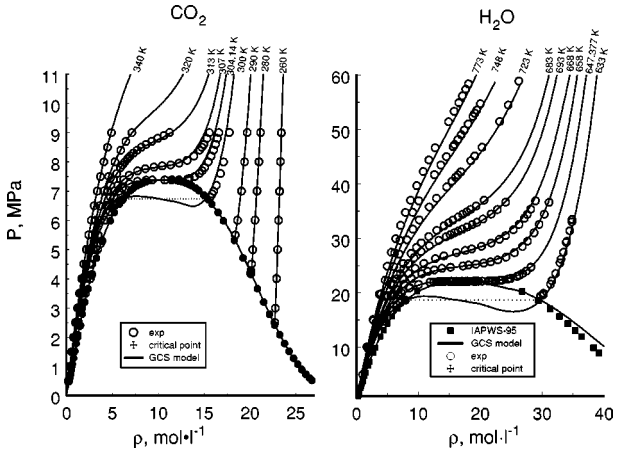


FIG. 2. $P\rho T$ data (symbols) for carbon dioxide—Refs. 139 and 140 (left) and water—Refs. 141–144 (right) with predictions of the GCS model (curves). The empty symbols correspond to the one-phase region, and the closed symbols indicate the VLE data.

densities in some monatomic fluids and methane with similar accuracy. But the DCS EOS exhibits fast deterioration of the quality of description of the saturated densities with increasing the carbon atoms in *n*-alkanes and is practically inapplicable for water and other polar and associated fluids. Besides, the DCS EOS, as well as all other analytical EOS, fails to reproduce the theoretically well-established asymptotic scaling laws in the critical region.

Since experimental data for methane, ethane, carbon dioxide, and water have been partially used for the optimization of the GCS model, it is not unexpected that the GCS model yields a good description of the thermodynamic surface in these fluids. From a practical point of view it is more interesting to test the GCS model against the PVT and VLE data for other fluids, which have not been used in the model optimization. In this work, we applied the GCS model for the prediction of the PVT and VLE properties of more than 30 pure fluids listed in Table I. In Fig. 3 we show the experimental saturated pressures and densities data for higher *n*-alkanes, up to *n*-eicosane ($C_{20}H_{42}$), in comparison with predictions of the GCS model. The dashed curves in Fig. 3 represent the values calculated with the CR SAFT EOS developed earlier for methane, ethane, *n*-hexane, *n*-decane, and *n*-eicosane by Kiselev and Ely.[76] For all *n*-alkanes, including *n*-eicosane, excellent agreement between the GCS model predictions and experimental data is observed. One can see from Fig. 3 that the GCS model without any adjustable parameters describes the PVT and VLE properties of *n*-alkanes practically with the same accuracy as the CR SAFT EOS

TABLE I. System-dependent constants for the GCS model.

| | $T_c$ (K) | $\rho_c$ (mol l$^{-1}$) | $Z_c$ | $\omega$ | $M_w$ |
|---|---|---|---|---|---|
| Methane | 190.564 | 10.122 | 0.286 773 | 0.0110 | 16.042 |
| Ethane | 305.322 | 6.8701 | 0.279 699 | 0.0994 | 30.069 |
| Propane | 369.850 | 5.0000 | 0.276 247 | 0.1520 | 44.097 |
| *n*-Butane | 425.160 | 3.9200 | 0.273 937 | 0.1930 | 58.124 |
| *n*-Pentane | 469.650 | 3.2155 | 0.266 800 | 0.2510 | 72.151 |
| *n*-Hexane | 507.850 | 2.7108 | 0.266 241 | 0.3000 | 86.178 |
| *n*-Heptane | 540.110 | 2.3352 | 0.260 327 | 0.3510 | 100.205 |
| *n*-Octane | 568.950 | 2.0310 | 0.259 166 | 0.3960 | 114.232 |
| *n*-Nonane | 594.550 | 1.8400 | 0.250 664 | 0.4440 | 128.259 |
| *n*-Decane | 617.650 | 1.6430 | 0.248 792 | 0.4882 | 142.284 |
| *n*-Eicosane | 767.300 | 0.8357 | 0.200 648 | 0.9070 | 282.556 |
| R12 | 385.010 | 4.6974 | 0.274 586 | 0.1795 | 120.910 |
| R134A | 374.274 | 5.0500 | 0.258 668 | 0.3270 | 102.300 |
| R22 | 369.320 | 5.9559 | 0.269 071 | 0.2210 | 120.910 |
| R32 | 351.350 | 8.2080 | 0.241 679 | 0.2770 | 52.0200 |
| R143A | 345.750 | 5.0810 | 0.257 761 | 0.2746 | 84.0440 |
| R125 | 339.330 | 4.7946 | 0.268 274 | 0.3030 | 120.020 |
| Methanol | 512.580 | 8.4746 | 0.224 213 | 0.5590 | 32.0420 |
| Ethanol | 516.250 | 5.9880 | 0.248 359 | 0.6350 | 46.0690 |
| Propan-1-ol | 536.710 | 4.5830 | 0.252 790 | 0.6240 | 60.0970 |
| Butan-1-ol | 562.900 | 3.6500 | 0.258 622 | 0.5900 | 74.1230 |
| Pentan-1-ol | 588.150 | 3.0300 | 0.263 949 | 0.5800 | 88.1500 |
| Hexan-1-ol | 611.400 | 2.6250 | 0.263 036 | 0.5600 | 102.177 |
| Heptan-1-ol | 633.150 | 2.2980 | 0.257 989 | 0.5600 | 116.204 |
| Octan-1-ol | 658.150 | 2.0430 | 0.267 270 | 0.5300 | 130.231 |
| Nonan-1-ol | 683.150 | 1.8370 | 0.256 367 | 0.5250 | 144.260 |
| Decan-1-ol | 705.100 | 1.6670 | 0.273 205 | 0.4840 | 158.390 |
| $CO_2$ | 304.128 | 10.625 | 0.274 588 | 0.2250 | 44.0100 |
| $H_2O$ | 647.096 | 17.874 | 0.229 450 | 0.3440 | 18.0158 |
| $D_2O$ | 643.847 | 17.776 | 0.227 750 | 0.3440 | 20.0275 |
| $N_2$ | 126.200 | 11.173 | 0.285 745 | 0.0400 | 28.0130 |
| $O_2$ | 154.580 | 13.623 | 0.284 424 | 0.0210 | 31.9990 |
| Ar | 150.660 | 13.395 | 0.291 369 | −0.004 | 39.9480 |

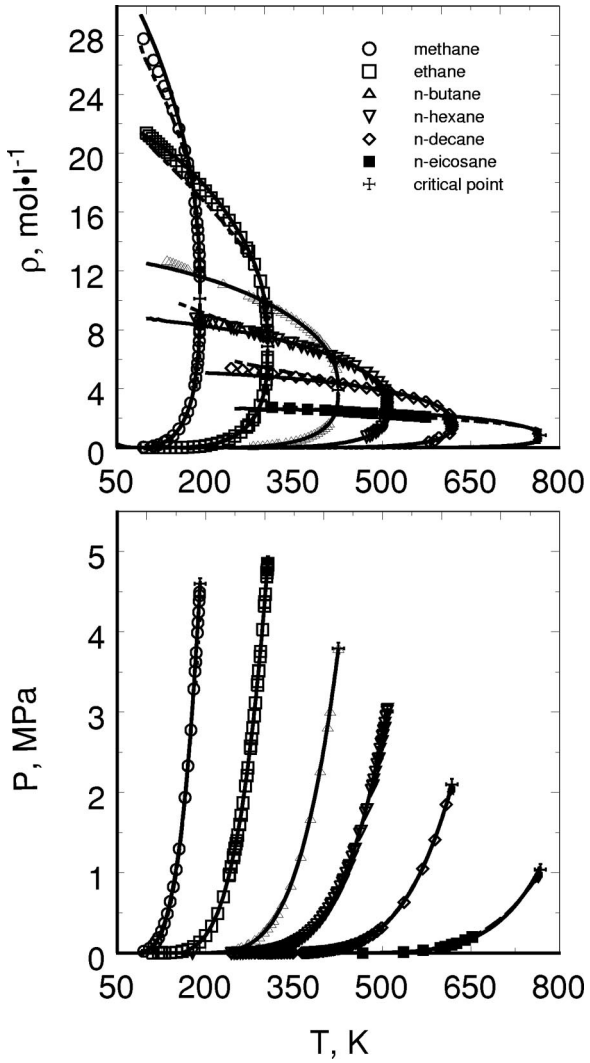


FIG. 3. The saturated density (top) and vapor pressure (bottom) data for methane (Ref. 135), ethane (Refs. 138, 145–148), *n*-butane (Refs. 147, 149–153), *n*-hexane (Refs. 154–163), *n*-decane (Refs. 164–174), and *n*-icosane—Ref. 175 (symbols) with predictions of the GCS model (solid curves) and the crossover SAFT EOS—Ref. 76 (dashed curves).

specially optimized to the experimental data for these substances.[76]

It is usually pointed out that a corresponding-states principle based only on the accentric factor $\omega$ is not applicable for polar and associating fluids.[111] Therefore, it is interesting to test the GCS model against experimental data for these fluids. One of the fluids, $H_2O$, was already considered earlier (see Fig. 2). A comparison of the predictions of the GCS model with the saturated pressure and density data for the hydro-fluorocarbons R12, R134A, R22, R32, R143A, and R125 is shown in Fig. 4, and in Figs. 5 and 6 for *n*-alcohols. In the entire temperature region $T_{tr} \leqslant T \leqslant T_c$, the GCS model reproduces the saturated pressures for all fluids shown in Figs. 3–5 with an AAD less than 1%. The GCS model also gives very good description of the saturated densities in and beyond the critical region. Some discrepancy between predicted and experimental values for liquid densities is observed only at low temperatures in R32 and methanol, where the GCS model predicts systematically lower (up to 5%)

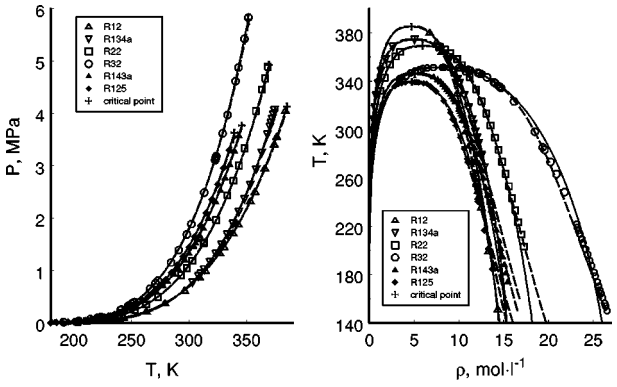


FIG. 4. The vapor pressure (left) and saturated density (right) data for hydrofluorocarbons R12 (Refs. 176–179), R134A (Refs. 180, 181), R22 (Refs. 182–184), R32 (Ref. 185), R143A (Ref. 186), and R125 (Refs. 187–189) (symbols) with predictions of the GCS model (solid curves) and the simplified crossover SAFT EOS—Ref. 78 (dashed curves).

values of the liquid densities than the experimental data (see Figs. 4 and 6). The dot-dashed curves in Fig. 6 correspond to the predictions of the simple CS model based on the crossover SAFT EOS.[79] As one can see, in the strong polar and associating fluids such as R32 and methanol the CR SAFT EOS[77–79] gives at low temperatures a better representation of the saturated liquid densities than the GCS model based on the simple cubic EOS. The AAD achieved with the GCS model for all data presented in Figs. 1–6 are summarized in Table II.

As it was pointed out earlier, although the six-term Landau model[59,62,63] and parametric crossover model[66–71,102] have a theoretical foundation in the renormalization-group theory and have been confirmed in the second order of $\varepsilon$ expansion, at $T<T_c$ they cannot be analytically extended deep into the metastable region. That restricts their application to the interface modeling and the surface tension calculations. As one can see from Figs. 1 and 2, the sine-model based GCS EOS, unlike the parametric crossover model[66–71,102] and cubic crossover EOS based on the LM equation for $\Upsilon$,[83] can be extended into the metastable region and at temperatures $T<T_c$ represents analytically connected van der Waals loops. This, together with the high accuracy of the representation of the PVT and VLE surface near to and far from the critical point, makes the GCS model extremely efficient for the direct interface and surface tension calculations.

## V. INTERFACE AND SURFACE TENSION

In the density-functional theory, the surface tension on the planar liquid–vapor interface is defined as[118,119]

$$\sigma = 2 \int_{-\infty}^{+\infty} c_0 \left( \frac{\partial \rho}{\partial z} \right)^2 dz, \tag{5.1}$$

where $\rho(z)$ is density of fluid at a distance $z$. The density profile $\rho(z)$ can be found from the optimization of the functional

$$\mathcal{F}[\rho(z)] = \int dr^2 \int [\hat{A}(\rho) + c_0 (\nabla \rho)^2] dz, \tag{5.2}$$

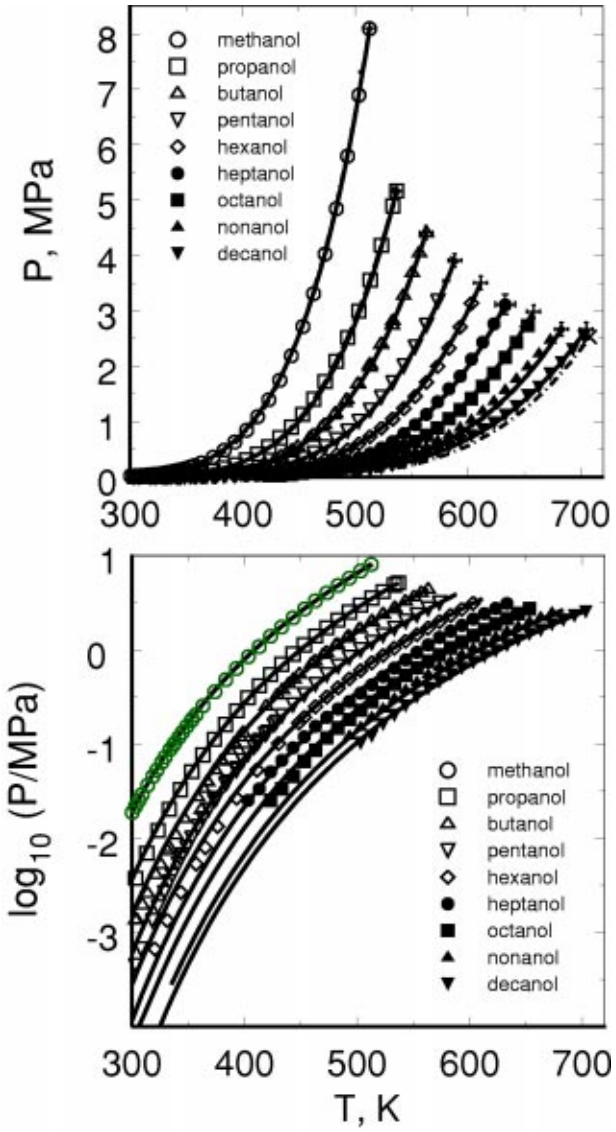


FIG. 5. The saturated pressure data in the normal (top) and logarithmic (bottom) scale for methanol (Refs. 190, 191), ethanol (Refs. 190, 192, 193), propan-1-ol (Refs. 190, 194), butan-1-ol (Refs. 190, 195), pentan-1-ol (Refs. 196–198), hexan-1-ol (Refs. 196–198), heptan-1-ol (Ref. 199), octan-1-ol (Ref. 200), nonan-1-ol (Ref. 200), and decan-1-ol—Ref. 200 (symbols) with predictions of the GCS model (solid curves), the crossover SAFT EOS—Ref. 77 (dashed curves), and crossover SAFT CS model—Ref. 79 (dot-dashed curves).

where $\hat{A}(\rho)=\rho A(T,\rho)$ is a Helmholtz free-energy density of the bulk fluid. Optimization of the functional (5.2) at condition $N=\text{const}$ by Langrange's method leads to the Euler–Lagrange equation

$$\frac{d\Delta\hat{A}(\rho)}{d\rho}-c_0\frac{d^2\rho}{dz^2}=0, \tag{5.3}$$

where $\Delta\hat{A}(\rho)=\hat{A}_b(T,\rho)-\rho\mu(T,\rho_{V,L})$ is an excess part of the Helmholtz free energy density, and $\mu(T,\rho_{V,L})=(\partial\rho A/\partial\rho)_T$ is a chemical potential of the bulk fluid along the saturated curve $\rho=\rho_{V,L}(T)$. The first integral of Eq. (5.3) is

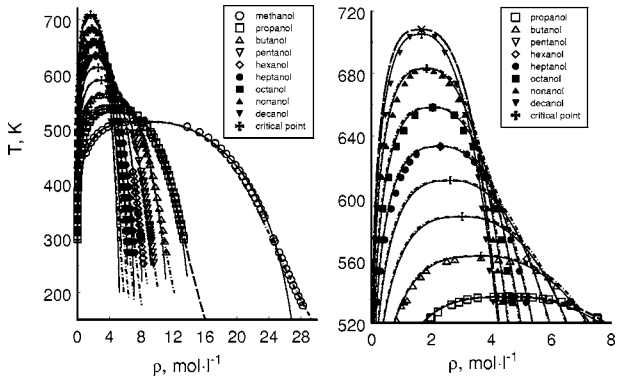


FIG. 6. The saturated density data for methanol (Refs. 190, 191, 201, 202), ethanol (Ref. 190), propan-1-ol (Refs. 190, 194), butan-1-ol (Refs. 200, 203), pentan-1-ol (Refs. 197, 204), hexan-1-ol (Refs. 196, 197, 205), heptan-1-ol (Ref. 199), octan-1-ol (Ref. 200), nonan-1-ol (Ref. 200), and decan-1-ol—Ref. 200 (symbols) with predictions of the GCS model (solid curves), the crossover SAFT EOS—Ref. 77 (dashed curves), and the crossover SAFT CS model—Ref. 79 (dot-dashed curves).

$$\frac{d\rho}{dz}=\left[\frac{\Delta\hat{A}(\rho)}{c_0}\right]^{1/2} \tag{5.4}$$

and the surface tension is given by

$$\sigma=c_0^{1/2}\int_{\rho_V}^{\rho_L}[\Delta\hat{A}(\rho)]^{1/2}d\rho. \tag{5.5}$$

In the Landau theory of inhomogeneous fluids,[15] the excess part of the free-energy density $\Delta\hat{A}$ is given by Eq. (2.1) where the order parameter $\eta=\rho/\rho_c-1$ and the ordering field $h=[\mu_b(T,\eta)-\mu_b(T,\rho_c)]/RT$, that leads to the MF expression for the surface tension

$$\sigma=\sigma_0|\tau|, \tag{5.6}$$

while in the scaling theory the asymptotic behavior of the surface tension in the critical region is given by[120]

$$\sigma=\sigma_0|\tau|^{2\nu}, \tag{5.7}$$

where $\nu\cong 0.63$ is a critical exponent of the correlation length.

In the CGS-DFT model developed in this work, we used Eq. (3.7) for the calculation of the excess free energy-density $\Delta\hat{A}(\rho)=\rho RT\Delta\overline{A}(T,\rho)$ with the parameters $\overline{\tau}$ and $\overline{\eta}$ as given by Eq. (3.4). The temperature dependence appears in the CGS-DFT model through the excess free-energy density $\Delta\hat{A}(\rho)$ and the parameter $c_0$. In our previous study[121,122] we

TABLE II. Percentage average absolute deviations (AAD %) between experimental data and values calculated with the GCS model.

| Region | Liquid densities | Vapor densities | Pressure |
|---|---|---|---|
| One-phase ($\rho\leqslant 2\rho_c$) | ··· | ··· | 1%–2% |
| Two-phase ($T_c>T>0.6T_c$) | 1%–2% | 2%–3% | 1% |
| Two-phase ($T<0.6T_c$) | 2%–3% | 3%–5% | 1%–2% |

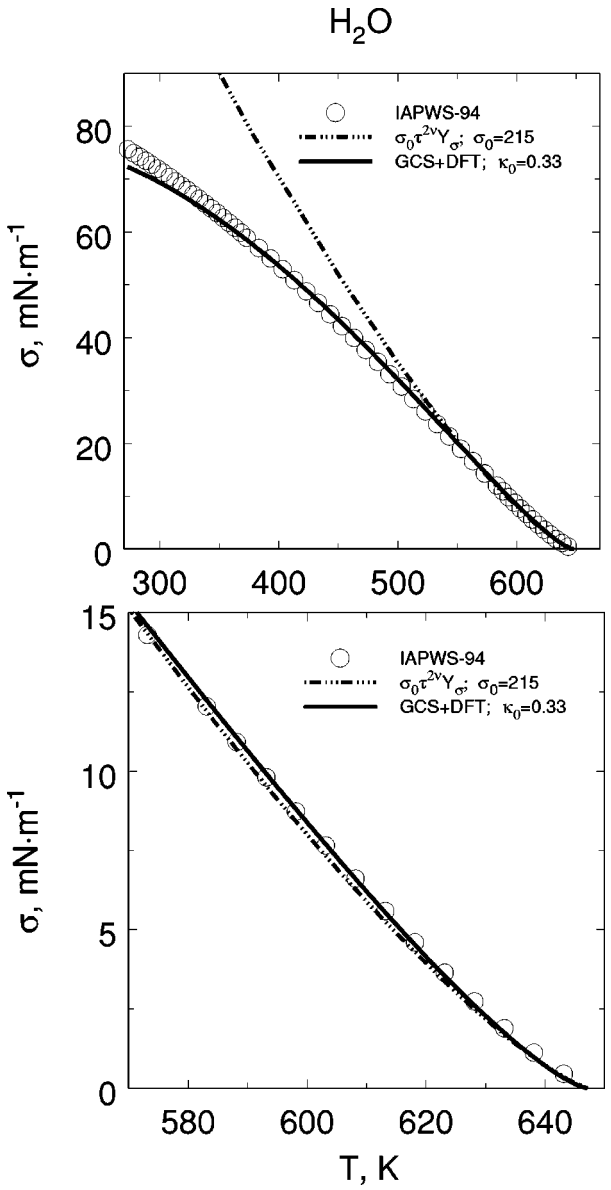


FIG. 7. The surface tension data for water—Ref. 123 (symbols) with predictions of the asymptotic crossover model by Belyakov *et al.*—Ref. 124 (dot-dashed curve), and GCS-DFT model (solid curve).

showed that for water, a good estimate for this parameter is $c_0 \cong k_B T \rho_c^{1/3}$. Following that study, for ordinary and heavy water we use here

$$c_0 = (1-\kappa_0)^2 k_B T \rho_c^{1/3}, \tag{5.8}$$

while for all other fluids we adopt the temperature-independent parameter $c_0$ in the form

$$c_0 = (1-\kappa_0)^2 k_B T_c \rho_c^{1/3}, \tag{5.9}$$

where $k_B$ is Boltzmann constant and the parameter $\kappa_0 < 1$ was introduced to take into account a difference of the prefactor $(1-\kappa_0)$ in real fluids from unity. Similar to the accentric factor $\omega$,[111] the coefficient $\kappa_0$ can be extracted from the surface tension measured at $T = 0.7 T_c$, or close values.

Because of the hydrogen bounding and strong oriental interaction between molecules, water is always a challenging object for modeling. In Fig. 7 we show a comparison of the

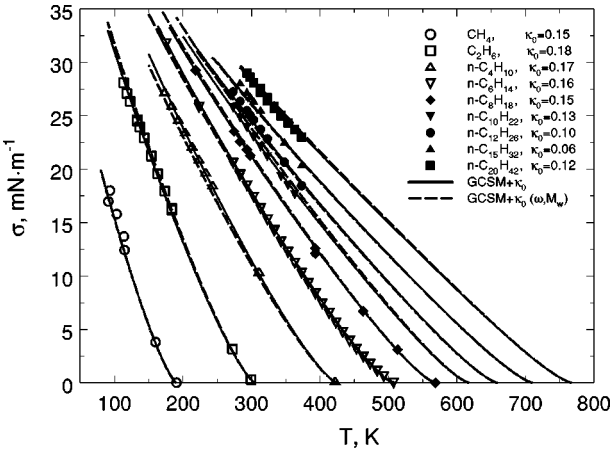


FIG. 8. The surface tension data (Ref. 206) for methane, ethane, *n*-hexane, *n*-octane, *n*-decane, *n*-dodecane, *n*-pentadecane, and *n*-icosane (symbols) with predictions of the GCS-DFT model (curves).

prediction of the GCS-DFT model for water with experimental data[123] and with the values calculated with the asymptotic crossover model developed earlier by Belyakov *et al.*[124] The latter one is a phenomenological generalization of the renormalization-group model, exact to the first order in the $\varepsilon$ expansion. This model contains the Ginzburg number as a parameter, and in the critical region (at $|\tau| \ll \mathrm{Gi}$), reproduces the scaling-law behavior (5.7) while at $\mathrm{Gi} \ll |\tau| \ll 1$ it corresponds to the MF Eq. (5.6). As one can see, in the critical region both models practically coincide and they both are in excellent agreement with experimental data. However, at low temperatures the asymptotic crossover model by Belyakov *et al.*[124] gives systematically higher values of the surface tension than experimental ones, while the GCS-DFT model follows experimental data with a high accuracy down to the temperature $T \simeq 300$ K. Only at low temperatures, $T \leqslant 300$ K, do systematic deviations of the GCS-DFT predictions from experimental data appear. These deviations are small (less than 3% at $T \simeq 273.16$ K) and we should contend that in general the GCS-DFT model yields an excellent representation of the surface tension in water.

In the case when no experimental data for surface tension are available, or the experimental information is scarce, for the estimation of the parameter $\kappa_0$ in nonionic and nonassociating fluids one can use a simple corresponding-state expression

$$\kappa_0 = 1.194 \times 10^{-2} M_w \left[ 1 - \frac{1.91 \omega^{1/2}}{(1+0.405\omega)^2} \right], \tag{5.10}$$

which appears to be a good approximation for *n*-alkanes (up to $C_{20}H_{42}$) and $CO_2$. In cryogenic liquids such as nitrogen and oxygen, Eq. (5.10) usually overestimates values for the parameter $\kappa_0$. Therefore, in order to provide a more reliable estimate for the surface tension in cryogenic liquids, a prefactor (1/3) should be applied to the parameter $\kappa_0$ calculated with Eq. (5.10). A comparison of the GCS-DFT model with surface-tension experimental data for several *n*-alkanes is shown in Fig. 8. The solid curves in Fig. 8 correspond to the values calculated with the parameter $\kappa_0$ extracted from the experimental data, while the dashed curves represent the pa-

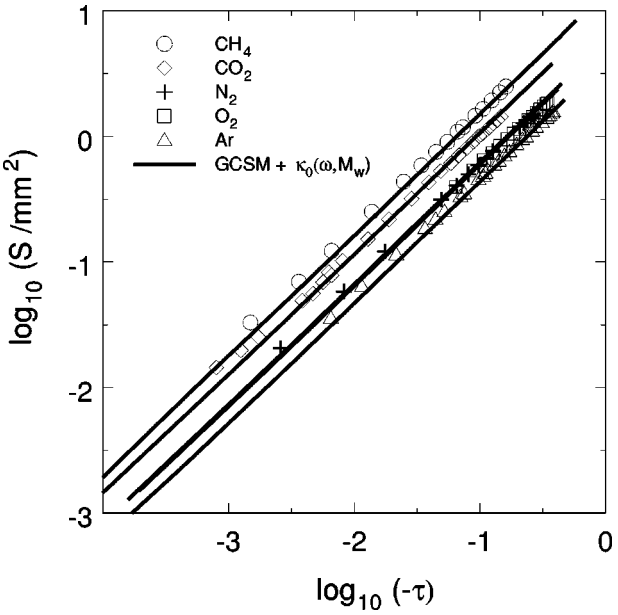


FIG. 9. The Sugden parameter data (Ref. 125) for methane, carbon dioxide, nitrogen, oxygen, and argon (symbols) with predictions of the GCS-DFT model (curves). For nitrogen, oxygen, and argon a pre-factor (1/3) in Eq. (5.10) for the parameter $\kappa_0$ was applied.

rameter $\kappa_0$ calculated with Eq. (5.10). As one can see, in both cases very good agreement between the GCS-DFT model and experimental data for all *n*-alkanes including *n*-eicosane ($C_{20}H_{42}$) is observed.

In Fig. 9 we show the predictions of the GCS-DFT model for the Sugden parameter

$$S=\frac{2\sigma}{g(\rho_L-\rho_V)} \tag{5.11}$$

(where $g$ is the acceleration due to the gravity) together with experimental data for $CH_4$, $CO_2$, $N_2$, $O_2$, and Ar obtained by Gielen *et al.*[125] Since the Sugden parameter involves simultaneous calculation of the surface tension and vapor–liquid densities, it is a good test for the physical self-consistency of the model in the critical region. Again, as one can see from Fig. 9, in the entire temperature region $T \leqslant T_c$ down to dimensionless temperatures of $(-\tau)\simeq 10^{-3}$ good agreement between experimental data and predicted values of the Sugden parameters is observed. The predictions of the asymptotic crossover model by Belyakov *et al.*[124] for the Sugden parameters are not shown in Fig. 9 because in the entire temperature range they practically coincide with the GCS-DFT curves.

## VI. EXTENSION OF THE GCS MODEL TO MIXTURES

In order to apply the GCS model to fluid mixtures, one needs to formulate the mixing rules for the system-dependent parameters of the model. For all classical EOS, these mixing rules are usually formulated in terms of composition $x$, that is physically correct far away from the critical point and can be justified by direct statistical mechanics calculations.[15] In the original PT EOS,[109,110] the coefficients $b$ and $c$ are simple linear functions of composition

$$b(x)=\sum_i b^{(i)}x_i, \quad c(x)=\sum_i c^{(i)}x_i, \tag{6.1}$$

where the index $i$ denotes the component of the mixture, and for the parameter $a$ the conventional van der Waals mixing rules are used. The critical parameters $T_c(x)$, $\nu_c(x)$, and $P_c(x)$ for binary mixtures are determined from the critical-point conditions[15]

$$\left(\frac{\partial\mu}{\partial x}\right)_{T_c,P_c}=0, \quad \left(\frac{\partial^2\mu}{\partial x^2}\right)_{T_c,P_c}=0, \quad \left(\frac{\partial^3\mu}{\partial x^3}\right)_{T_c,P_c}>0, \tag{6.2}$$

where $\mu=\mu_2-\mu_1=(\partial A/\partial x)_{T,\nu}$ is the chemical potential of a mixture. Using general thermodynamic relations (see Appendix B), the conditions (6.2) can be represented in the form[56]

$$\left(\frac{\partial P}{\partial \nu}\right)_{T_c,\mu_c}=0, \quad \left(\frac{\partial^2 P}{\partial \nu^2}\right)_{T_c,\mu_c}=0, \quad \left(\frac{\partial^3 P}{\partial \nu^3}\right)_{T_c,\mu_c}>0, \tag{6.3}$$

which determine $T_c(x)$, $\nu_c(x)$, and the chemical potential $\mu_c(x)$ of a mixture. Comparing these conditions with the corresponding conditions for one-component fluids [see Eq. (A3)] one can conclude that in the critical region the equation of state of binary mixtures at fixed chemical potential has the same analytic form as, or is isomorphic to, the EOS of one-component fluids.[56] In a more general formulation, the principle of critical-point universality[53–55] means that with adding into the system a density variable $x_i$ the thermodynamic potential of mixtures

$$\tilde{A}(T,\nu,\mu_{i=1,2,\ldots,n})=\overline{A}(T,\nu,x_{i=1,2,\ldots,n})-\sum_{i=1}^{n}\tilde{\mu}_i x_i \tag{6.4}$$

at fixed field variable $\tilde{\mu}_i=\mu_i/RT$, related to composition $x_i=-(\partial\tilde{A}/\partial\tilde{\mu}_i)_{T,\nu,m_{j\neq i}}$, has the same analytical form as the thermodynamic potential of a one-component fluid $A(T,\nu)$. Therefore, in order to reproduce the nonanalytical singular behavior of binary mixtures in the critical region one should consider the thermodynamic potential $\tilde{A}(T,\nu,\tilde{\mu})$, rather than the Helmholtz free energy $\overline{A}(T,\nu,x)$. It means, that for the physically self-consistent representation of the thermodynamic surface of fluid mixtures close to and far away from the critical region, not only a crossover EOS for pure components, but also the field-variable (FV) mixing rules should be used.

In this work, we developed for binary mixtures the GCS-FV model formulated in terms of the field variable $\tilde{x}=\exp(\tilde{\mu})/[1+\exp(\tilde{\mu})]$, which related to the composition through the thermodynamic relation

$$x=-\tilde{x}(1-\tilde{x})\left(\frac{\partial\tilde{A}}{\partial\tilde{x}}\right)_{T,\nu}. \tag{6.5}$$

For the thermodynamic potential $\tilde{A}$ we use in the GCS-FV model the GCS model for pure fluids as determined by Eqs. (3.7), and (4.2)–(4.8), but with the molecular weight and accentric factor expressed as linear functions of the field variable $\tilde{x}$,

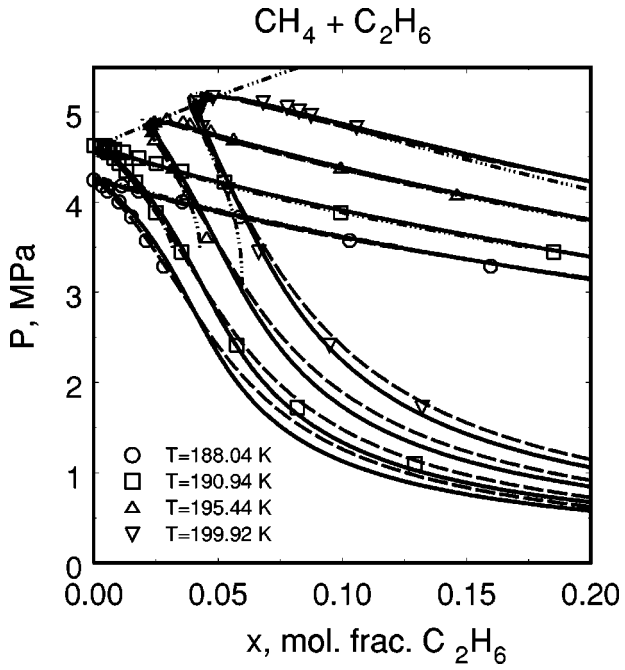


FIG. 10. VLE data for methane+ethane mixtures by Wichterle and Kobayashi (Ref. 207) in comparison with values calculated with the GCS-FV model (solid curves), CREOS-97 (dot–dashed curevs), and the GCS-XV model (long-dashed curves).

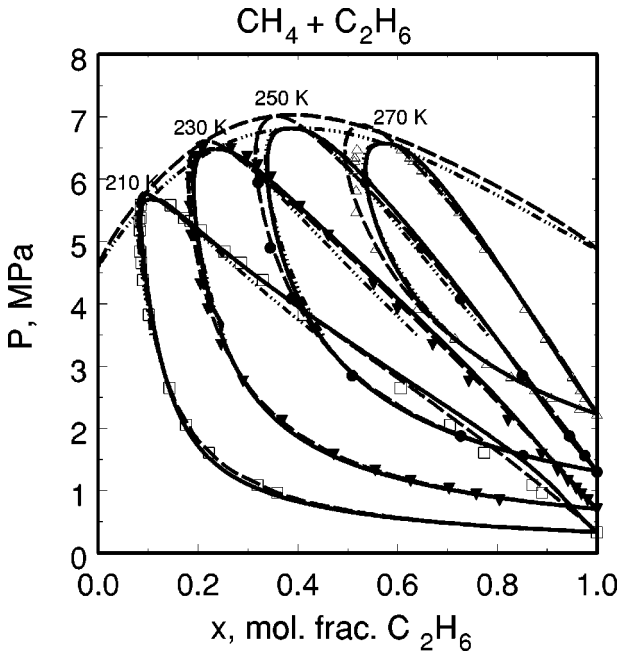


FIG. 11. VLE data for methane+ethane mixtures by Wei *et al.* (Ref. 128) in comparison with values calculated with the GCS-FV model (solid curves), CREOS-97—Ref. 67 (dot–dashed curves), and the GCS-XV model (long-dashed curves).

$$M_w(x)=\sum_i M_w^{(i)}\tilde{x}_i, \quad \omega(x)=\sum_i \omega^{(i)}\tilde{x}_i. \tag{6.6}$$

Since in the nonreacting systems the zero level of the entropy $S_0=-dA^{\mathrm{id}}/dT|_{T\to 0}$ can be chosen arbitrary, the temperature dependent ideal gas part of the Helmholtz free energy for binary mixtures $\overline{A}^{\mathrm{id}}(T)=\overline{A}_1^{\mathrm{id}}(T)(1-x)+\overline{A}_2^{\mathrm{id}}(T)x$ is usually considered without a linear term $\propto T$. In this work, we consider the ideal gas part $\tilde{A}^{\mathrm{id}}(T,\tilde{x})$ for the GCS-FV model in the form

$$\frac{\tilde{A}^{\mathrm{id}}(T,\tilde{x})}{RT}=\ln(1-\tilde{x})+\tilde{a}_0(\tilde{x})+\tilde{a}_1(\tilde{x})\tau(\tilde{x}) +\overline{A}_1^{\mathrm{id}}(T)(1-\tilde{x})+\overline{A}_2^{\mathrm{id}}(T)\tilde{x}, \tag{6.7}$$

where $\tau(\tilde{x})=T/T_c(\tilde{x})-1$ is a dimensionless deviation of the temperature from the critical temperature $T_c(\tilde{x})$ at fixed field variable $\tilde{x}$ and the coefficient $\tilde{a}_0$ is determined from the so-called critical line condition (CLC)

$$\frac{d\tilde{a}_0}{d\tilde{x}}=\frac{d\Delta\tilde{A}_{\mathrm{bg}}}{d\tilde{x}}+\frac{\tilde{a}_1}{T_c}\frac{dT_c}{d\tilde{x}} =-\frac{\nu_c}{v_{0c}^2}\frac{d\nu_{0c}}{d\tilde{x}}\overline{P}_0(T_c)+\Delta\nu_c\left(\frac{d\overline{P}_0}{d\tilde{x}}\right)_{T=T_c}+\left(\frac{d\tilde{A}_0^{\mathrm{res}}}{d\tilde{x}}\right)_{T=T_c} +\overline{A}_1^{\mathrm{id}}(T_c)-\overline{A}_2^{\mathrm{id}}(T_c)+\frac{\tilde{a}_1}{T_c}\frac{dT_c}{d\tilde{x}}, \tag{6.8}$$

where $\Delta\tilde{A}_{\mathrm{bg}}=\tilde{A}_{\mathrm{bg}}-\ln(1-\tilde{x})$. The CLC, first introduced by Moldover and Gallagher[126] and later modified by Rainwater[127] for the Leung–Griffiths model and by Kiselev *et al.*[66,70] for the CREOS-97, implies that a zero level of the entropy of a binary mixture can be chosen so that the field variable $\tilde{x}=x$ not only in the pure component limits ($x=0$ and $x=1$), but also along the whole critical locus $T_c(\tilde{x})=T_c(x)$ and $\nu_c(\tilde{x})=\nu_c(x)$. With the CLC given by Eq. (6.8), a general thermodynamic relation (6.5) can be written in the form

$$x=\tilde{x}-\tilde{x}(1-\tilde{x})\left[\left(\frac{\partial\Delta\tilde{A}}{\partial\tilde{x}}\right)_{T,\nu}+\left(\frac{\partial\tilde{A}_{\mathrm{bg}}}{\partial\tilde{x}}\right)_{T,\nu} +\frac{d\Delta\tilde{A}_{\mathrm{bg}}}{d\tilde{x}}+\left(\frac{d\tilde{a}_1}{d\tilde{x}}-\frac{\tilde{a}_1}{T_c}\frac{dT_c}{d\tilde{x}}\right)\tau(\tilde{x})\right] \tag{6.9}$$

that provides in the GCS-FV model a relationship between $x$ and $\tilde{x}$ at given $T$ and $\nu$.

In this work, we applied the GCS-FV model to the prediction of the VLE surface in methane+ethane mixture. In the GCS-FV model for methane+ethane mixtures we adopted the same critical locus as obtained earlier by Kiselev in the CREOS-97,[66] while for the parameter $\tilde{a}_1$ we use a simple linear function

$$\tilde{a}_1(\tilde{x})=\tilde{\alpha}_1+\tilde{\alpha}_2\tilde{x}, \tag{6.10}$$

where the coefficients $\tilde{\alpha}_1=0.53$ and $\tilde{\alpha}_2=-3.65$ have been found from a fit of the model to the few low-pressure VLE data points at $T=230$ K obtained by Wei *et al.*[128] Comparisons of the GCS-XV model with experimental VLE data for methane+ethane mixtures are shown in Figs. 10 and 11. The dot-dashed lines in Figs. 10 and 11 represent the values calculated with the CREOS-97[66] and the long-dashed curves correspond to the GCS-XV model with the mixing rules formulated in terms of composition. In the GCS-XV model, the

coefficients $b(x)$ and $c(x)$ were calculated with Eq. (6.1), while for the coefficient $a(T)$ we used the modified van der Waals mixing rules in the form[83]

$$a_{0c}(x)=\sum_i x_i \sum_j x_j \sqrt{a_{0c}^{(i)}(T_{0c})a_{0c}^{(j)}(T_{0c})}(1-k_{ij}),$$
$$k_{ij}=k_{ji}, \quad k_{ii}=k_{jj}=0, \tag{6.11}$$

where a temperature-dependent function $\alpha_a(T)$ is calculated with Eq. (4.2), the accentric factor

$$\omega(x)=\sum_i \omega^{(i)}x_i, \tag{6.12}$$

and the pseudocritical parameters $T_{0c}(x)$ and $\nu_{0c}(x)$, and the critical compressibility $Z_{0c}(x)$ are determined by Eq. (A2) with the coefficients $\Omega_a$, $\Omega_b$, and $\Omega_c$ given in the Appendix [see Eqs. (A6) and (A9)]. The coefficient $k_{12}=-1.63\times10^{-2}$ for this mixture was found from a fit of the GCS-XV model to the PVT-data obtained by Haynes *et al.*[129] and by Bespalov *et al.*[130] As one can see from Figs. 10 and 11, in the critical region the GCS-FV model practically coincides with the CREOS-97, while far away from the critical region it is close to the GCS-XV model. The GCS-XV yields very good representation of the VLE surface at low pressures and compositions, but on moderate compositions, the GCS-XV predicts in the critical region the systematically higher pressures than experimental data and values calculated with the CREOS-97.[66]

In this work, we also applied the GCS-FV model for the prediction of the VLE surface in the carbon dioxide+ethane mixture, which contains a critical azeotrope, and, therefore, is interesting for testing of the GCS-XV model. For the carbon dioxide+ethane mixture we used the critical locus obtained by Kiselev and Kulikov,[68] while the coefficients $\tilde{\alpha}_1=2$ and $\tilde{\alpha}_2=-2.7$ have been found from an optimization of the model to the few VLE-data points obtained at $T=263.15$ K by Brown *et al.*[131] A comparison of the predictions of the GCS-FV model with experimental data in carbon dioxide+ethane mixtures is shown in Fig. 12. Again, a very good agreement of the GCS-FV model with all experimental data in the entire temperature range from critical locus down $T=223.15$ K is observed. At low temperatures (at $T\leqslant270$ K) the GCS-FV model even gives a better representation of the VLE surface in carbon dioxide+ethane mixtures than the parametric crossover model.[68] In the critical region at $T\geqslant283$ K both models practically coincide.

The compositions of the vapor and liquid phases in binary mixtures usually do not coincide, while the field variable $\tilde{x}$ has the same value in both phases. Therefore, the VLE surface in binary mixtures by definition belongs to the isomorphic path $\tilde{x}=$const. This means that for calculation of the surface tension in a binary mixture one can use Eq. (5.5), but with the excess free energy-density calculated at $\tilde{x}=$const with the corresponding GCS-FV model. We are not aware of any experimental surface-tension data for methane+ethane and carbon dioxide+ethane mixtures, therefore, in Fig. 13 we show the predicted values of the surface tension against experimental data for carbon dioxide—*n*-butane mixtures.[132] In the GCS-FV model data for carbon dioxide—*n*-butane mixtures, we adopted the same critical locus as employed earlier by Kiselev and Rainwater,[67] while parameters $\tilde{\alpha}_1=1$ and $\tilde{\alpha}_2=-4$ were determined from an optimization to a few bubble-curve data points at $T=319.3$ K.[132] As one can see, at this isotherm excellent agreement between experimental data and GCS-FV+DFT predictions is observed. At lower temperatures, the GCS-FV model predicts the systematically lower values of the surface tension than experimental data, but in general an agreement between theory and experiment is fairly good. The dashed curve in Fig. 13 represents the values with two-scale-factor-universality (TSFU) model by Sahimi and Taylor.[133] Since both models, GCS-FV+DFT and TSFU, are based on the principle of the critical-point universality it is interesting to compare the predictions of the TSFU model for the surface tension in carbon dioxide—*n*-butane mixtures with our calculations. As one can see from Fig. 13, in the critical region both models give very similar predictions.

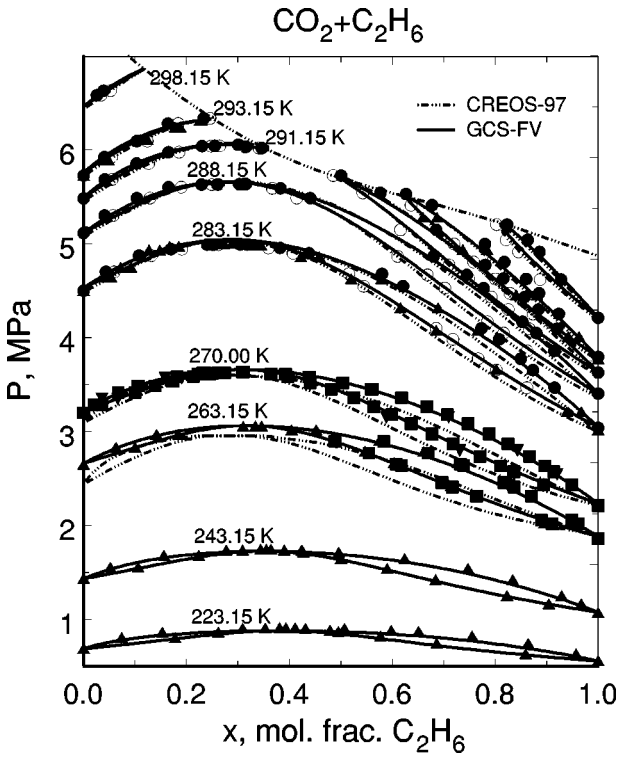


FIG. 12. VLE data for carbon dioxide+ethane mixtures (Refs. 128, 131, 208, 209) (symbols) in comparison with values calculated with the GCS-FV model (solid curves) and with the parametric crossover EOS by Kiselev and Kulikov—Ref. 68 (dot-dashed curves).

## VII. CONCLUSION

In this paper, we describe a general approach for developing a ''global'' crossover EOS, which in the critical region reproduces theoretically well-established scaling laws, and in the limit of low densities is transformed into the ideal gas equation. Using a simple cubic EOS as a reference EOS for one-component fluids, we developed a generalized corresponding state model for pure fluids and fluid mixtures, which in addition to the accentric factor $\omega$ contains also the Ginzburg Gi as a parameter. In general, the Ginzburg number

is independent CS parameters, but for nonionic and nonpolymeric fluids we expressed Gi as a simple function of the classical CS parameters, $\omega$ and $Z_c$, and the molecular weight $M_w$, thus formally reducing the number of the input parameters in the GCS model to two. Unlike all other ''global'' crossover models developed before, the GCS model was formulated in the closed analytical form and at temperatures $T < T_c$ can be extended into the metastable region for representing analytically connected van der Waals loops. This allowed us to develop on the basis of the GCS model and the density functional theory a generalized CS-DFT model for the volumetric properties, VLE-surface, and surface tension. The GCS-DFT model requires only the critical parameters $T_c$, $P_c$, $\rho_c$, and the accentric factor $\omega$ as input, but represents the $P\rho T$ and VLE data, as well as the surface tension of one-component fluids (polar and nonpolar) in a wide range, including the nearest vicinity of the critical point, with a high accuracy. In the critical region, the GCS-DFT model reproduces all theoretical scaling laws for the liquid–vapor densities, surface tension, and the Sugden parameter.

In spite of the obvious advantage of the GCS model over all other ''global'' EOS developed earlier, it also has a shortcoming in describing the saturated liquid densities for strong polar and associating fluids at low temperatures. We found that for these fluids the crossover SAFT EOS developed in our previous papers[76–79] yields better results than the GCS model. However, we need to note that the problem appears in the range of temperatures and densities where the crossover function $\Upsilon \cong 1$ and, therefore, is not specific to the GCS model only, but is rather a ''genetic'' defect of all cubic EOS in general. At low temperatures, the crossover SAFT EOS in agreement with experimental data yields an almost linear temperature-dependence for the saturated liquid densities, while the CR LCS, similar to all classical cubic EOS, gives a parabolic-like dependence. Therefore, in order to improve the representation of the low-temperature liquid-densities data for strong polar and associating fluids, the reference cubic EOS in the GCS model should be replaced on the SAFT EOS, as the most promising one.

In this work, we also extended the GCS model to binary mixtures. Using the principle of the critical point universality we developed the GCS-FV model with all system parameters expressed as functions of the field variable $\tilde{x}$. We compare this model with experimental data for methane+ethane and carbon dioxide+ethane mixtures and with the GCS-XV model formulated in terms of composition $x$. The GCS-FV model developed in this work reproduces the VLE surface of binary in the critical region with the same accuracy as the CREOS-97,[66] and far away from the critical point the GCS-FV model reproduces the VLE data with the same accuracy as the GCS-XV model, while the GCS-XV model fails to reproduce the critical locus of mixture with experimental accuracy and predicts in the critical region systematically higher values of pressure than experimental ones.

We should point out that the goal of this work was not to develop a new, more accurate EOS for some particular mixtures, and the methane+ethane and carbon dioxide+ethane mixtures have been chosen only as examples. The major objective of this work was to develop a generalized but still simple CS model, which is able to predict the thermodynamic surface and interface in pure fluids and fluid mixtures with high accuracy. Therefore, for the coefficient $\tilde{a}_1(\tilde{x})$ we used the simplest linear relation (6.10) with the parameters determined from the low-temperature low-pressure VLE data for each mixture. In this case, the GCS-FV gives in the one phase region at $\rho \geqslant 1.65\rho_c$ systematically lower values of pressure than experimental data, and we anticipate that this simple linear relation for the mixing coefficient $\tilde{a}_1(\tilde{x})$ can also cause some problems in the extension of the GCS-FV model to multicomponent and more complex mixtures with volatile and nonvolatile components. As an example we considered here the surface tension in $CO_2+n$-butane mixture (see Fig. 13). At low temperatures and compositions the GCS+DFT model does predict systematically lower values of the surface tension than experimental ones. This can be partially explained because the critical locus by Kiselev and Rainwater[67] does not correspond exactly to the experimental critical locus by Hsu *et al.*,[132] and because Eq. (6.10) for this system should be replaced with other more accurate correlation. The isomorphic corresponding-states expression formulated in terms of the excess compressibility factor $\Delta Z_c(\tilde{x})$[66,70] is a good candidate for this replacement, among other options.

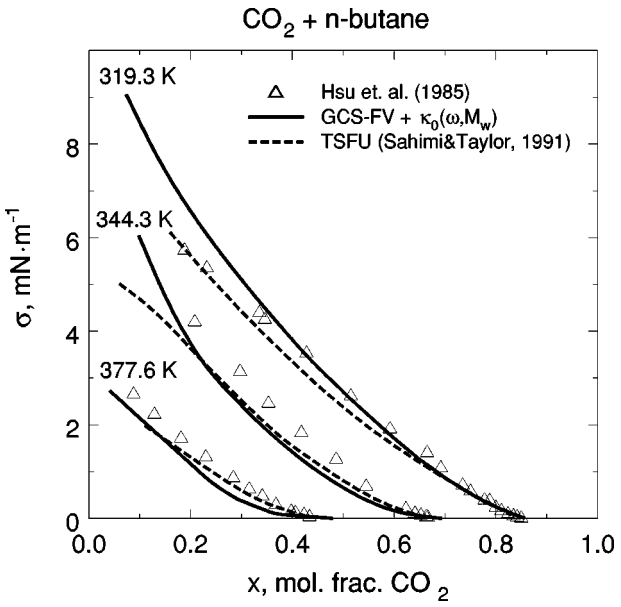


FIG. 13. The surface tension data (Ref. 132) for $CO_2+n$-butane mixtures (symbols) with predictions of the GCS-FV+DFT model (solid curves) and the TSFU model (dashed curves) by Sahimi and Taylor (Ref. 133).

The GCS-DFT model is based on the renormalization-group and density functional theories and, therefore, except for the reference EOS, does not contain any restriction on its application to other systems with the scalar order parameter. This generality of the GCS model allows us also to apply this model for the analysis of the phase behavior of much more complex systems than simple fluids and their binary mixtures. Recently Elliott and co-workers[134] presented experimental ISiS data for the excited nuclei, which have been interpreted by the authors as the liquid–vapor equilibrium of finite neutral nuclear matter. Comparisons of experimental

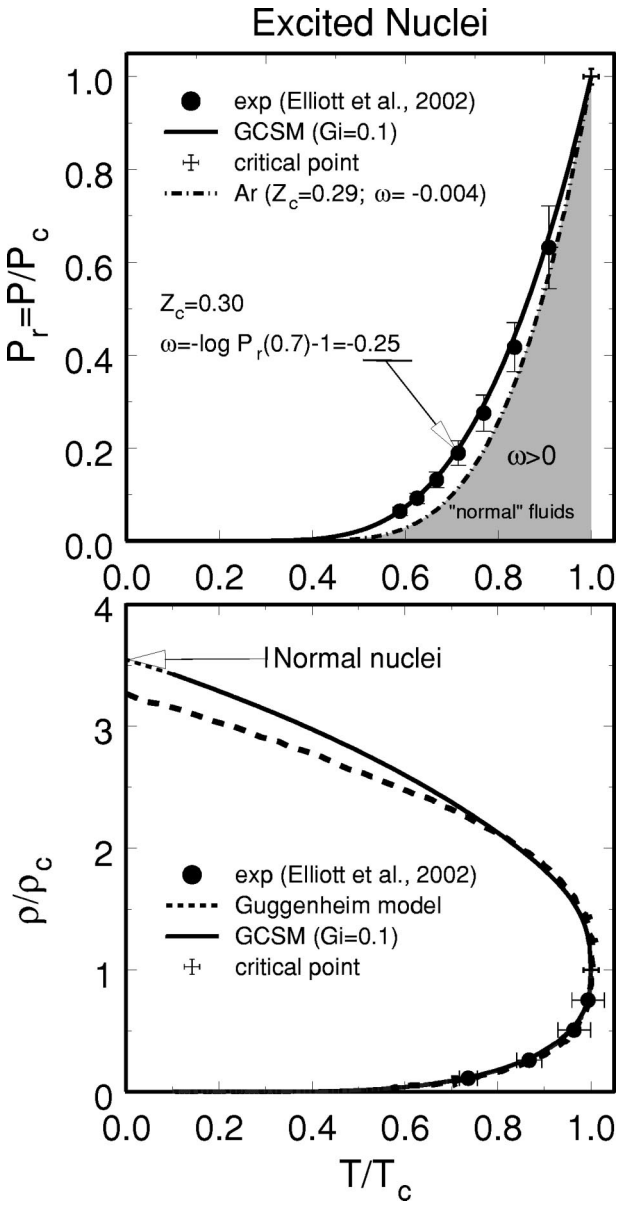


FIG. 14. The vapor pressure (top) and saturated density (bottom) data for finite neutral nuclear matter—Ref. 134 (symbols) with predictions of the GCS model (solid curves) and Guggenheim model—Ref. 134 (dashed curves). The dot-dashed curve represents the values of saturated pressures calculated with the GCS model for argon ($\omega=-0.004$) and the shaded area corresponds to "normal" fluids with $\omega\geqslant 0$.

data obtained by Elliott *et al.*[134] with the predictions of the GSM model are shown in Fig. 14. The shaded area in Fig. 14 marks the region, which corresponds to "normal" fluids with $\omega\geqslant 0$. As one can see, with $\omega=-0.25$ and $Z_c=0.3$ extracted from the experimental data,[134] and with the Ginzburg number $\mathrm{Gi}=0.1$, which was considered in this case as an independent CS parameter, the predictions of the GCS model are in excellent agreement with experimental data. We consider this result as additional conformation of the conclusion made by Elliott and co-workers[134] that experimental data in the excited nuclei can be really treated as liquid–vapor equilibrium of finite neutral nuclear matter, but with enormously small, negative accentric factor $\omega$.

Currently there is a growing interest in modeling of the thermodynamic surface, interface properties, and wetting transitions in such systems as polymers and polymer solutions, surfactants, and micro emulsions. We do believe that successful solution of this problem is possible only after comprehensive understanding of the physical nature of these phenomena and developing an adequate model for their describing. We are not aware of any other theoretical model, with the same degree of simplicity, physical self-consistency, and accuracy of representation of the thermodynamic and surface properties of fluid systems close in and far beyond the critical region as the GCS-DFT model. Therefore, we consider this work as an important step in this direction. Research toward the application of the GCS model to the bulk properties and interface, as well as adsorption and wetting transitions in more complex fluid systems is now in progress and the results will be presented in future publications.

## ACKNOWLEDGMENTS

The authors are indebted to J. Jechura for providing us with his modified version of the PT EOS prior to publication. The research was supported by the U.S. Department of Energy, Office of Basic Energy Sciences, under the Grant No. DE-FG03-95ER14568.

## APPENDIX A: PATEL–TEJA EQUATION OF STATE

The Patel–Teja (PT) EOS[109,110] can be written in the form

$$P=\frac{RT}{\nu-b}-\frac{a}{\nu(\nu+b)+c(\nu-b)}, \tag{A1}$$

where $P$ is the pressure, $\nu=1/\rho$ is molar volume, and $R$ is the universal gas constant,

$$\begin{aligned} a(T)&=\Omega_a\frac{R^2T_{0c}^2}{P_{0c}}\alpha_a(T)=a_{0c}\alpha_a(T),\\ b&=\Omega_b\frac{R^2T_{0c}}{P_{0c}},\quad c=\Omega_c\frac{RT_{0c}}{P_{0c}}, \end{aligned} \tag{A2}$$

where $\alpha_a(T)=\alpha_a(T_r)$ is a function of the dimensionless temperature $T_r=T/T_{0c}$ with an asymptotic value $\alpha_a(1)=1$, the coefficients $\Omega_a$, $\Omega_b$, and $\Omega_c$ are functions of the critical compressibility $Z_{0c}$, and the classical critical parameters $T_{0c}$, $P_{0c}$, and $\nu_{0c}$ that can be found from the condition

$$\left(\frac{\partial P}{\partial\nu}\right)_{T_{0c}}=0,\quad \left(\frac{\partial^2 P}{\partial\nu^2}\right)_{T_{0c}}=0,\quad \frac{P_{0c}\nu_{0c}}{RT_{0c}}=Z_{0c}\leqslant\frac{1}{3}. \tag{A3}$$

In the dimensionless form, the PT EOS is given by[74]

$$\overline{P}=\frac{P\nu_{0c}}{RT}=\frac{1}{\nu_r-(\Omega_b/Z_{0c})}-\frac{\Omega_a}{Z_{0c}T_r}\frac{\alpha_a(T_r)}{(\nu_r+\hat{\Omega}_1)(\nu_r+\hat{\Omega}_2)} \tag{A4}$$

and the residual Helmholtz free energy

$$\overline{A}_0^{\rm res}(T) = -\ln\left(\nu_r - \frac{\Omega_b}{Z_{0c}}\right) + \frac{\Omega_a}{Z_{0c}}\frac{\alpha_a(T_r)}{T_r}\ln\left(\frac{\nu_r+\hat{\Omega}_1}{\nu_r+\hat{\Omega}_2}\right), \tag{A5}$$

where $T_r = T/T_{0c}$, $\nu_r = \nu/\nu_{0c}$, the parameters $\Omega_a$, $\hat{\Omega}_1$, and $\hat{\Omega}_2$, are given by

$$\Omega_a = 3Z_{0c}^2 + 3(1-2Z_{0c})\Omega_b + \Omega_b^2 + \Omega_c, \qquad \Omega_c = 1 - 3Z_{0c}, \tag{A6}$$

$$\hat{\Omega}_1 = (\Omega_c + \Omega_b - \Omega)/2Z_{0c}, \quad \hat{\Omega}_2 = (\Omega_c + \Omega_b + \Omega)/2Z_{0c}, \tag{A7}$$

$$\Omega = \sqrt{\Omega_c^2 + \Omega_b^2 + 6\Omega_c\Omega_b}, \tag{A8}$$

and $\Omega_b$ is the smallest positive root of the cubic equation

$$\Omega_b^3 + (2-3Z_{0c})\Omega_b^2 + 3Z_{0c}^2\Omega_b - Z_{0c}^3 = 0. \tag{A9}$$

Along the critical isochore, $\nu_r = 1$, the pressure

$$\overline{P}_0(T) = \frac{1}{1-(\Omega_b/Z_{0c})} - \frac{\Omega_a}{Z_{0c}T_r}\frac{\alpha_a(T_r)}{(1+\hat{\Omega}_1)(1+\hat{\Omega}_2)}, \tag{A10}$$

and the residual Helmholtz free energy

$$\overline{A}_0^{\rm res}(T) = -\ln\left(1 - \frac{\Omega_b}{Z_{0c}}\right) + \frac{\Omega_a}{Z_{0c}}\frac{\alpha_a(T_r)}{T_r}\ln\left(\frac{1+\hat{\Omega}_1}{1+\hat{\Omega}_2}\right). \tag{A11}$$

## APPENDIX B: CRITICAL POINT CONDITIONS IN BINARY MIXTURES

At $N = \text{const}$ the critical point conditions in binary mixtures are given by[15]

$$\left(\frac{\partial\mu_2}{\partial x}\right)_{P,T} = 0, \quad \left(\frac{\partial^2\mu_2}{\partial x^2}\right)_{P,T} = 0, \quad \left(\frac{\partial^3\mu_2}{\partial x^3}\right)_{P,T} > 0. \tag{B1}$$

The chemical potentials of the mixture components

$$\mu_1 = \phi - x\left(\frac{\partial\phi}{\partial x}\right)_{P,T}, \quad \mu_2 = \phi + (1-x)\left(\frac{\partial\phi}{\partial x}\right)_{P,T}, \tag{B2}$$

where $\phi = \Phi/N$ is the Gibbs energy per mole, the derivatives $(\partial\phi/\partial x)_{P,T} = (\partial A/\partial x)_{T,\nu} = \mu$, and the first equality in Eq. (B1) takes the form

$$\left(\frac{\partial\mu_2}{\partial x}\right)_{P,T} = \left(\frac{\partial^2\phi}{\partial x^2}\right)_{P,T} = \left(\frac{\partial^2 A}{\partial x^2}\right)_{T,\nu} + \left(\frac{\partial^2 A}{\partial x\partial\nu}\right)_T\left(\frac{\partial\nu}{\partial x}\right)_{P,T} = \left(\frac{\partial\mu}{\partial x}\right)_{T,\nu} + \left(\frac{\partial P}{\partial x}\right)_{T,\nu}^2\left(\frac{\partial\nu}{\partial P}\right)_{T,x} = 0. \tag{B3}$$

Using the thermodynamic relations $(\partial\mu/\partial x)_{T,\nu} = (\partial P/\partial x)_{T,\nu}(\partial\nu/\partial x)_{T,\mu}$ and $(\partial P/\partial\nu)_{T,\mu} = (\partial P/\partial\nu)_{T,x} + (\partial P/\partial x)_{T,\nu}(\partial x/\partial\nu)_{T,\mu}$ one can rewrite Eq. (B3) in the form

$$\left(\frac{\partial\mu}{\partial x}\right)_{T,\nu}\left(\frac{\partial\nu}{\partial P}\right)_{T,x}\left(\frac{\partial P}{\partial\nu}\right)_{T,\mu} = \left(\frac{\partial\nu}{\partial x}\right)_{P,T}\left(\frac{\partial\nu}{\partial x}\right)_{T,\mu}\left(\frac{\partial P}{\partial\nu}\right)_{T,\mu} = 0, \tag{B4}$$

or the same $(\partial P/\partial\nu)_{T_c,\mu_c} = 0$. Similarly, one can show that the second equality in Eq. (B1) is equivalent to the condition $(\partial^2 P/\partial\nu^2)_{T_c,\mu_c} = 0$.


[1] *Supercritical Fluid Technology: Reviews in Modern Theory and Application*, edited by T. J. Bruno and J. F. Ely (CRS, Boston, 1991).
[2] P. T. Anastas and T. C. Williamson, ACS Symp. Ser. **1**, 626 (1996).
[3] B. Horton, Nature (London) **400**, 797 (1999).
[4] D. Adam, Nature (London) **407**, 938 (2000).
[5] M. Modell, in *Standard Handbook of Hazardous Waste Treatment and Disposal*, edited by H. M. Freeman (McGraw–Hill, New York, 1989), p. 8.153.
[6] J. W. Tester, H. R. Holgate, F. J. Armellini, P. Webley, W. R. Killilea, G. T. Hong, and H. E. Barner, in *Emerging Technologies in Hazardous Waste Managment III.*, edited by D. W. Tedder and F. G. Pohland (American Chemical Society, Washington, DC, 1993), Chap. 3.
[7] E. F. Gloyna and L. Li, Environ. Prog. **14**, 182 (1995).
[8] A. S. Zakharov, V. V. Kachalov, S. B. Kiselev, A. V. Chernomyrdin, and E. E. Shpilrain, High Temp. **35**, 96 (1997).
[9] M. Polikoff and S. Howdle, Chem. Ber. **31**, 118 (1995).
[10] P. E. Savage, S. Gopalan, T. L. Mizan, C. J. Martino, and E. E. Brook, AIChE J. **47**, 1723 (1995).
[11] H. Black, Environ. Sci. Technol. **30**, 124A (1996).
[12] D. A. Morgenstern, R. M. LeLacheur, D. K. Morita, S. L. Borowsky, S. Feng, G. H. Brown, L. Luan, M. F. Gross, M. J. Burk, and W. Tumas, ACS Symp. Ser. **626**, 132 (1996).
[13] D. Weinstein, A. R. Renslo, R. L. Danheiser, and J. W. Tester, J. Phys. Chem. B **103**, 2878 (1999).
[14] J. D. van der Waals and F. Kohnstamm, *Lehrbuch der Thermostatic*, (Verlag von Johann Amrosius Barth, Leipzing, 1927), Vol. 2.
[15] L. D. Landau and E. M. Lifshitz, *Statistical Physics*, (Pergamon, New York, 1980), Part 1.
[16] O. Redlich and J. N. S. Kwong, Chem. Rev. **44**, 233 (1949).
[17] G. Soave, Chem. Eng. Sci. **27**, 1197 (1972).
[18] D. Y. Peng and D. B. Robinson, Ind. Eng. Chem. Fundam. **15**, 59 (1976).
[19] A. Anderko, in *Equations of State for Fluids and Fluid Mixtures*, edited by J. V. Sengers, R. F. Kayser, C. J. Peters, and H. J. J. White (Elsevier, Amsterdam, 2000), Part I, pp. 75–126.
[20] J. V. Sengers and J. M. H. Levelt Sengers, Annu. Rev. Phys. Chem. **37**, 189 (1986).
[21] M. A. Anisimov, S. B. Kiselev, J. V. Sengers, and S. Tang, Physica A **188**, 487 (1992).
[22] J. R. Fox, Fluid Phase Equilib. **14**, 45 (1983).
[23] J. R. Fox and T. S. Strovick, Int. J. Thermophys. **11**, 61 (1990).
[24] A. Parola and L. Reatto, Phys. Rev. Lett. **53**, 2417 (1984).
[25] A. Parola and L. Reatto, Phys. Rev. A **31**, 3309 (1985).
[26] A. Parola, A. Meroni, and L. Reatto, Int. J. Thermophys. **10**, 345 (1989).
[27] M. Tau, A. Parola, D. Pini, and L. Reatto, Phys. Rev. E **52**, 2644 (1995).
[28] L. Reatto and A. Parola, J. Phys.: Condens. Matter **8**, 9221 (1996).
[29] D. Pini, A. Parola, and L. Reatto, Int. J. Thermophys. **19**, 1545 (1998).
[30] D. Pini, G. Stell, and N. B. Wilding, Mol. Phys. **95**, 483 (1998).
[31] P. C. Albright, J. V. Sengers, J. F. Nicoll, and M. Ley-Koo, Int. J. Thermophys. **7**, 75 (1986).
[32] A. Kostrowichka Wysolkovska, M. A. Anisimov, and J. V. Sengers, Fluid Phase Equilib. **158–160**, 523 (1999).
[33] A. van Pelt, G. X. Jin, and J. V. Sengers, Int. J. Thermophys. **15**, 687 (1994).
[34] D. D. Erikson and T. W. Leland, Int. J. Thermophys. **7**, 911 (1986).
[35] J. J. De Pablo and J. M. Prausnitz, Fluid Phase Equilib. **59**, 1 (1990).
[36] J. A. White and S. Zhang, J. Chem. Phys. **103**, 1922 (1990).
[37] J. A. White and S. Zhang, J. Chem. Phys. **99**, 2012 (1993).
[38] J. A. White, J. Chem. Phys. **111**, 9352 (1999).
[39] J. A. White, J. Chem. Phys. **112**, 3236 (2000).
[40] J. A. White, Int. J. Thermophys. **22**, 1147 (2001).
[41] T. Kraska and U. K. Deiters, Int. J. Thermophys. **15**, 261 (1994).
[42] T. Kraska, J. Supercrit. Fluids **16**, 1 (1999).
[43] Y. Tang, J. Chem. Phys. **109**, 5935 (1998).
[44] L. Lue and J. M. Praustitz, J. Chem. Phys. **108**, 5529 (1998).
[45] L. Lue and J. M. Praustitz, AIChE J. **44**, 1455 (1998).
[46] F. Fornasiero, L. Lue, and A. Bertucco, AIChE J. **45**, 906 (1999).
[47] J. Jiang and J. M. Prausnitz, J. Chem. Phys. **111**, 5964 (1999).
[48] J. Jiang and J. M. Prausnitz, Fluid Phase Equilib. **169**, 127 (2000).
[49] J. Jiang and J. M. Prausnitz, AIChE J. **46**, 2525 (2000).
[50] J. M. H. Levelt Sengers, J. Chang, and G. Morrison, in *Equation of*

*State—Theory and Applications*, edited by K. C. Chao and D. B. Robinson, Jr., ACS Symposium Series 300 (ACS, Columbus, Ohio, 1986), pp. 110–131.
[51] M. A. Anisimov and S. B. Kiselev, in *Soviet Technology Review B Thermal Physics Reviews, Part 2*, edited by A. E. Scheindlin and V. E. Fortov (Harwood Academic, New York, 1992), Vol. 3, pp. 1–121.
[52] M. A. Anisimov and J. V. Sengers, in *Equations of State for Fluids and Fluid Mixtures*, edited by J. V. Sengers, R. F. Kayser, C. J. Peters, and H. J. White, Jr. (Elsevier, Amsterdam, 2000), pp. 382–433.
[53] M. Fisher, Phys. Rev. **176**, 257 (1968).
[54] W. F. Saam, Phys. Rev. A **2**, 1461 (1970).
[55] R. B. Griffiths and J. C. Wheeler, Phys. Rev. A **2**, 1047 (1970).
[56] M. A. Anisimov, A. V. Voronel, and E. E. Gorodetskii, Sov. Phys. JETP **33**, 605 (1971).
[57] M. A. Anisimov, E. E. Gorodetskii, V. D. Kulikov, A. A. Povodyrev, and J. V. Sengers, Physica A **220**, 277 (1995).
[58] J. R. Fox and T. S. Strovick, Int. J. Thermophys. **11**, 49 (1990).
[59] G. X. Jin, S. Tang, and J. V. Sengers, Phys. Rev. E **47**, 388 (1993).
[60] A. A. Povodyrev, G. X. Jin, S. B. Kiselev, and J. V. Sengers, Int. J. Thermophys. **17**, 909 (1996).
[61] S. B. Kiselev and A. A. Povodyrev, High Temp. **34**, 621 (1996).
[62] A. Kostrowichka Wysolkovska and J. V. Sengers, J. Chem. Phys. **111**, 1551 (1999).
[63] K. S. Abdulkadirova, A. Kostrowicka Wyczalkovska, M. A. Anisimov, and J. V. Sengers, J. Chem. Phys. **116**, 4597 (2002).
[64] M. Y. Belyakov, S. B. Kiselev, and J. C. Rainwater, J. Chem. Phys. **107**, 3085 (1997).
[65] S. B. Kiselev, M. Y. Belyakov, and J. C. Rainwater, Fluid Phase Equilib. **150**, 439 (1998).
[66] S. B. Kiselev, Fluid Phase Equilib. **128**, 1 (1997).
[67] S. B. Kiselev and J. C. Rainwater, Fluid Phase Equilib. **141**, 129 (1997).
[68] S. B. Kiselev and V. D. Kulikov, Int. J. Thermophys. **18**, 1143 (1997).
[69] S. B. Kiselev, J. C. Rainwater, and M. L. Huber, Fluid Phase Equilib. **150–151**, 469 (1998).
[70] S. B. Kiselev and J. C. Rainwater, J. Chem. Phys. **109**, 643 (1998).
[71] S. B. Kiselev and M. L. Huber, Int. J. Refrig. **21**, 64 (1998).
[72] S. B. Kiselev and J. F. Ely, J. Chem. Phys. **116**, 5657 (2002).
[73] S. B. Kiselev and J. F. Ely, J. Chem. Phys. **118**, 680 (2003).
[74] S. B. Kiselev, Fluid Phase Equilib. **147**, 7 (1998).
[75] L. Kudelkova, J. Lovland, and P. Vonka, Fluid Phase Equilib. (in press).
[76] S. B. Kiselev and J. F. Ely, Ind. Eng. Chem. Res. **38**, 4993 (1999).
[77] S. B. Kiselev, J. F. Ely, H. Adidharma, and M. Radosz, Fluid Phase Equilib. **183–184**, 53 (2000).
[78] S. B. Kiselev and J. F. Ely, Fluid Phase Equilib. **174**, 93 (2000).
[79] S. B. Kiselev, J. F. Ely, I. M. Abdulagatov, and J. W. Magee, Int. J. Thermophys. **6**, 1373 (2000).
[80] Z.-Q. Hu, J.-C. Yang, and Y.-G. Li, Fluid Phase Equilib. **205**, 1 (2003).
[81] Z.-Q. Hu, J.-C. Yang, and Y.-G. Li, Fluid Phase Equilib. **205**, 25 (2003).
[82] S. B. Kiselev, J. F. Ely, L. Lue, and J. R. Elliott, Jr., Fluid Phase Equilib. **200**, 121 (2002).
[83] S. B. Kiselev and D. G. Friend, Fluid Phase Equilib. **162**, 51 (1999).
[84] A. Z. Patashinskii and V. L. Pokrovskii, *Fluctuation Theory of Phase Transitions*, 1st ed. (Pergamon, New York, 1979).
[85] J. Rudnick and D. R. Nelson, Phys. Rev. B **13**, 2208 (1976).
[86] A. D. Bruce and D. J. Wallace, J. Phys. Chem. A **9**, 1117 (1976).
[87] J. F. Nicoll, Phys. Rev. A **24**, 2203 (1981).
[88] J. F. Nicoll and J. K. Bhattacharjee, Phys. Rev. B **23**, 389 (1981).
[89] J. F. Nicoll and P. C. Albright, Phys. Rev. B **31**, 4576 (1985).
[90] J. F. Nicoll and P. C. Albright, Phys. Rev. B **34**, 1991 (1986).
[91] C. Bagnuls and C. Bervillier, Phys. Rev. B **27**, 6995 (1983).
[92] C. Bagnuls and C. Bervillier, Phys. Rev. B **32**, 7209 (1985).
[93] C. Bagnuls, C. Bervillier, D. I. Meiron, and B. G. Nickel, Phys. Rev. B **35**, 3585 (1987).
[94] M. Y. Belyakov and S. B. Kiselev, Physica A **190**, 75 (1992).
[95] M. Campostrini, A. Pelisseto, P. Rossi, and E. Vicari, Phys. Rev. E **60**, 3526 (1999).
[96] S. Caracciolo, M. S. Causo, A. Pelisseto, P. Rossi, and E. Vicari, Nucl. Phys. B (Proc. Suppl.) **73**, 757 (1999).
[97] A. Pelisseto, P. Rossi, and E. Vicari, Nucl. Phys. B **554**, 552 (1999).
[98] S. Caracciolo, M. S. Causo, A. Pelisseto, P. Rossi, and E. Vicari, Phys. Rev. E **64**, 046130 (2001).
[99] F. J. Wegner, Phys. Rev. B **5**, 4529 (1972).
[100] S. B. Kiselev, High Temp. **28**, 42 (1990).
[101] S. B. Kiselev, I. G. Kostyukova, and A. A. Povodyrev, Int. J. Thermophys. **12**, 877 (1991).
[102] S. B. Kiselev and J. V. Sengers, Int. J. Thermophys. **14**, 1 (1993).
[103] Z. Y. Chen, A. Abbaci, S. Tang, and J. V. Sengers, Phys. Rev. A **42**, 4470 (1990).
[104] Z. Y. Chen, P. C. Albright, and J. V. Sengers, Phys. Rev. A **41**, 3161 (1990).
[105] S. Tang, J. V. Sengers, and Z. Y. Chen, Physica A **179**, 344 (1991).
[106] M. Fisher and G. Orkoulas, Phys. Rev. Lett. **85**, 696 (2000).
[107] G. Orkoulas, M. E. Fisher, and A. Z. Panagiotopoulos, Phys. Rev. E **63**, 051507 (2001).
[108] J. M. H. Levelt Sengers, in *Supercritical Fluid Technology: Reviews in Modern Theory and Applications*, edited by J. F. Bruno and T. J. Ely (CRC Press, Boca Raton, FL, 1991).
[109] N. C. Patel and A. S. Teja, Chem. Eng. Sci. **37**, 463 (1982).
[110] N. C. Patel, Int. J. Thermophys. **17**, 673 (1996).
[111] C. R. Reid, J. M. Prausnitz, and B. E. Polling, *The Properties of Gases and Liquids*, 4th ed. (McGraw–Hill, New York, 1987).
[112] S. M. Walas, *Phase Equilibrium in Chemical Engineering* (Butterworth, Boston, 1985).
[113] M. Fisher, S.-Y. Zinn, and P. Upton, Phys. Rev. B **59**, 14533 (1999).
[114] J. A. Barker and D. Henederson, Rev. Mod. Phys. **48**, 587 (1976).
[115] J. F. Ely and I. M. F. Marrucho, in *Equations of State for Fluids and Fluid Mixtures, Part I*, edited by J. V. Sengers, R. F. Kayser, C. J. Peters, and H. J. White, Jr. (Elsevier, Amsterdam, 2000), pp. 289–358.
[116] J. Jechura (privite communication).
[117] R. J. Sadus, J. Chem. Phys. **115**, 1460 (2001).
[118] J. S. Rowlinson and B. Widom, *Molecular Theory of Capillarity* (Clarendon, Oxford, 1982).
[119] H. T. Davis, *Statistical Mechanics of Phases, Interphases, and Thin Films* (VCH, New York, 1996).
[120] B. Widom, J. Chem. Phys. **43**, 3892 (1965).
[121] S. B. Kiselev and J. F. Ely, Physica A **299**, 357 (2001).
[122] S. B. Kiselev, Physica A **269**, 252 (1999).
[123] *IAPWS Release on Surface Tension of Ordinary Water Substance September 1994* (IAPWS, Orlando, FL, 1994).
[124] M. Y. Belyakov, S. B. Kiselev, and A. R. Muratov, High Temp. **33**, 701 (1995).
[125] H. L. Gielen, O. B. Verbeke, and J. Thoen, J. Chem. Phys. **81**, 6154 (1984).
[126] M. R. Moldover and J. S. Gallagher, AIChE J. **24**, 268 (1978).
[127] J. C. Rainwater, in *NIST Technical Note 1328* (USGPO, Washington, DC, 1989).
[128] M. S.-W. Wei, T. S. Brown, A. J. Kidnay, and E. D. Sloan, J. Chem. Eng. Data **40**, 726 (1995).
[129] W. M. Haynes, R. D. McCarty, and B. E. Eaton, J. Chem. Thermodyn. **17**, 209 (1985).
[130] M. D. Bespalov, V. B. Nagaev, V. A. Smirnov, and S.-E. Khalidov, Telplofiz. Svoystva Veschestv Mater. (Russian) **27**, 32 (1989).
[131] T. S. Brown, A. J. Kidnay, and E. D. Sloan, Fluid Phase Equilibria **40**, 169 (1988).
[132] J. J.-C. Hsu, N. Nagarajan, and L. Robinson, Jr., J. Chem. Eng. Data **30**, 485 (1985).
[133] M. Sahimi and B. N. Taylor, J. Chem. Phys. **95**, 6749 (1991).
[134] J. B. Elliott, L. G. Moretto, L. Phair *et al.*, Phys. Rev. Lett. **88**, 042701 (2002).
[135] R. Kleinrahm, W. Duschek, and W. Wagner, J. Chem. Thermodyn. **18**, 1103 (1986).
[136] R. Kleinrahm, W. Duschek, and W. Wagner, J. Chem. Thermodyn. **24**, 685 (1992).
[137] A. Van Itterbeek, O. Verbeke, and K. Staes, Physica (Utrecht) **29**, 742 (1963).
[138] D. R. Douslin and R. H. Harrison, J. Chem. Thermodyn. **5**, 491 (1973).
[139] W. Duschek, R. Kleinrahm, and W. Wagner, J. Chem. Thermodyn. **22**, 827 (1990).
[140] R. Gilgen, R. Kleinrahm, and W. Wagner, J. Chem. Thermodyn. **24**, 1243 (1992).
[141] S. L. Rivkin and T. S. Akhundov, Teploenergetika (Russian) **9**, 57 (1962).
[142] S. L. Rivkin and T. S. Akhundov, Teploenergetika (Russian) **10**, 66 (1963).
[143] S. L. Rivkin and G. V. Troyanovskaya, Teploenergetika (Russian) **11**, 72 (1964).
[144] S. L. Rivkin, T. S. Akhundov, E. A. Kremenevskaya, and N. N. Asadullaeva, Teploenergetika (Russian) **13**, 59 (1966).

[145] C. H. Barkkelew, J. L. Valentine, and C. O. Hurd, Am. Inst. Chem. Eng. Symp. Ser. **43**, 25 (1947).
[146] A. K. Pal, G. A. Pope, Y. Arai, N. F. Carnahan, and R. Kobayashi, J. Chem. Eng. Data **21**, 394 (1976).
[147] W. M. Haynes and M. J. Hiza, J. Chem. Thermodyn. **9**, 179 (1977).
[148] R. D. Goodwin, H. M. Roder, and G. S. Straty, Natl. Bur. Stand. (U.S.), Technical Note 684 (1976).
[149] L. J. Dana, A. C. Jenkins, J. N. Burdick, and R. C. Timm, Refr Eng. **12**, 387 (1926).
[150] B. H. Sage, D. C. Webster, and W. N. Lacey, Ind. Eng. Chem. **29**, 1309 (1937).
[151] J. F. Connolly, Ind. Eng. Chem. **48**, 813 (1956).
[152] J. F. Connolly, J. Phys. Chem. **66**, 1082 (1962).
[153] W. Kay, Ind. Eng. Chem. **32**, 358 (1940).
[154] D. S. Kurumov and B. A. Grigoryev, Russ. J. Phys. Chem. **56**, 338 (1986).
[155] J. L. Daridon, B. Lagourette, and J.-P. E. Grolier, Int. J. Thermophys. **19**, 145 (1998).
[156] J. A. Ellis and K. C. Chao, J. Chem. Eng. Data **18**, 264 (1973).
[157] J. Genco, A. Teja, and W. Kay, J. Chem. Eng. Data **25**, 355 (1980).
[158] W. B. Kay, R. Hoffman, and O. Davies, J. Chem. Eng. Data **20**, 333 (1975).
[159] A. H. N. Mousa, J. Chem. Thermodyn. **9**, 1063 (1977).
[160] P. Sauermann, K. Holzapfel, and T. W. DeLoos, Fluid Phase Equilib. **112**, 249 (1995).
[161] J. Shim and J. P. Kohn, J. Chem. Eng. Data **7**, 3 (1962).
[162] G. L. Thomas and S. Young, J. Chem. Soc. **67**, 1071 (1895).
[163] S. A. Wieczorek and J. Stecki, J. Chem. Thermodyn. **10**, 177 (1978).
[164] M. Gehrig and H. Lentz, Erdoel Kohle-Erdgas Petrochem. **36**, 277 (1983).
[165] E. Alcart, G. Tardajos, and M. D. Pena., **105**, 79 (1981).
[166] N. Allemand, J. Jose, and J. C. Merlin, Thermochim. Acta **105**, 79 (1986).
[167] J. M. Beaudoin and J. P. Kohn, J. Chem. Eng. Data **12**, 189 (1967).
[168] G. F. Carruth and R. Kobayashi, J. Chem. Eng. Data **18**, 115 (1973).
[169] R. D. Chirico, A. Nguyen, W. V. Steele, M. M. Strube, and C. Tsonopoulos, J. Chem. Eng. Data **34**, 149 (1989).
[170] R. W. Dornte and C. P. Smyth, J. Am. Chem. Soc. **52**, 3546 (1930).
[171] A. W. Francis, Ind. Eng. Chem. Fundam. **49**, 1779 (1957).
[172] J. Gregorowicz, K. Kiciak, and S. Malanowski, Fluid Phase Equilib. **38**, 97 (1987).
[173] H. H. Reamer, R. H. Olds, B. H. Sage, and W. N. Lacey, Ind. Eng. Chem. **34**, 1526 (1942).
[174] C. B. Willingham, W. J. Taylor, J. M. Pignocco, and F. D. Rossini, J. Res. Natl. Bur. Stand. **35**, 219 (1945).
[175] A. K. Doolittle, Ind. Eng. Chem. Res. **9**, 275 (1964).
[176] L. F. Kells, S. R. Orfeo, and W. H. Mears, Refr Eng. **63**, 46 (1955).
[177] K. Watanabe, T. Tanaka, and K. Oguchi, in Seventh ASME Thermophysical Properties Conference, edited by A. Cezarliyan, Gaithersburg, MD, 1977, pp. 470–479.
[178] E. Fernandez-Fassnacht and F. Del Rio, Cryogenics **25**, 204 (1985).
[179] R. C. McHarness, B. J. Eiseman, and J. J. Martin, Refr Eng. **63**, 31 (1955).
[180] H. D. Baehr and R. Tillner-Roth, J. Chem. Thermodyn. **23**, 1063 (1991).
[181] G. Morrison and D. K. Ward, Fluid Phase Equilib. **62**, 65 (1991).
[182] M. Zander, in the Fourth ASME Thermophysics Symposium, edited by J. R. Moszynski, Gaithersburg, MD, 1968, pp. 114–123.
[183] L. M. Lagutina, Kholodilnaya Tekhnika (Russian) (Refrigerant Techniques) **43**, 25 (1966).
[184] M. Okada, M. Uematsu, and K. Watanabe, J. Chem. Thermodyn. **18**, 527 (1986).
[185] P. F. Malbrunot, P. A. Meunier, G. M. Scatena, W. H. Mears, K. P. Murphy, and J. V. Sinka, J. Chem. Eng. Data **13**, 16 (1968).
[186] M. McLinden, Div. 838.08, NIST, Boulder CO (private communication).
[187] J. W. Magee, Int. J. Thermophys. **17**, 803 (1996).
[188] D. R. Defibaugh and G. Morrison, Fluid Phase Equilib. **80**, 157 (1992).
[189] S. Kuwubara, H. Aoyama, H. Sato, and K. Watanabe, J. Chem. Eng. Data **40**, 112 (1995).
[190] D. Ambrose and C. H. Sprake, J. Chem. Thermodyn. **2**, 631 (1970).
[191] W. E. Donham, Ph.D. thesis, Ohio State University, 1953.
[192] A. F. Gallaugher and H. Hibbert, J. Am. Chem. Soc. **59**, 2514 (1937).
[193] K. P. Mischenko and V. V. Subbotina, J. Appl. Chem. USSR **40**, N5 (1967).
[194] A. J. Kubicek and P. T. Eubank, J. Chem. Eng. Data **17**, 232 (1972).
[195] N. B. Vargaftik (Hemisphere, 1975), p. 767.
[196] R. C. Wilhoit and B. J. Zwolinski, J. Phys. Chem. Ref. Data **2**, Suppl. 1 (1973).
[197] K. R. Hall, Thermodynamics Research Center, Texas A&M University, College Station, TX, 1980.
[198] D. R. Stull, Ind. Eng. Chem. **39**, 517 (1947).
[199] K. R. Hall, Thermodynamics Research Center, Texas A&M University, College Station, TX, 1987.
[200] Y. V. Efremov, Russ. J. Phys. Chem. **40**, 1240 (1966).
[201] V. G. Komarenko, V. G. Manzhelii, and A. V. Radtsig, Ukr. Fiz. Zh. (Russ. Ed.) **12**, 681 (1967).
[202] E. W. Washburn, *International Critical Tables of Numerical Data, Physics, Chemistry, and Technology* (McGraw–Hill, New York, 1926).
[203] D. Ambrose and R. Townsend, J. Chem. Soc. **37**, 3614 (1963).
[204] J. L. Hales and J. H. Ellender, J. Chem. Thermodyn. **8**, 1177 (1976).
[205] J. Ortega, J. Chem. Eng. Data **30**, 5 (1985).
[206] N. B. Vargaftik, *Handbook of Physical Properties of Liquids and Gases*, 2nd ed. (Hemisphere, Washington, 1983).
[207] V. Wichterle and R. Kobayashi, J. Chem. Eng. Data **17**, 726 (1972).
[208] A. Fredenslund and J. Mollerup, J. Chem. Soc. Faraday Trans. I **70**, 1653 (1974).
[209] K. Ogaki and T. Katayama, Fluid Phase Equilib. **1**, 27 (1992).